

Quantum Encoding and Analysis on Continuous Stochastic Process

Xi-Ning Zhuang,^{1,2} Zhao-Yun Chen,³ Cheng Xue,³ Yu-Chun Wu,^{2,4,5,3,*} and Guo-Ping Guo^{2,4,5,3,1,†}

¹*Origin Quantum Computing, Hefei, China*

²*CAS Key Laboratory of Quantum Information, University of Science and Technology of China, Hefei, 230026, China*

³*Institute of Artificial Intelligence, Hefei Comprehensive National Science Center*

⁴*CAS Center for Excellence and Synergistic Innovation Center in Quantum Information and Quantum Physics, University of Science and Technology of China, Hefei, 230026, China*

⁵*Hefei National Laboratory, University of Science and Technology of China, Hefei 230088, China*

The continuous time stochastic process is a mainstream mathematical instrument modeling the random world with a wide range of applications involving finance, statistics, physics, and time series analysis, while the simulation and analysis of the continuous time stochastic process is a challenging problem for classical computers. In this work, a general framework is established to prepare the path of a continuous time stochastic process in a quantum computer efficiently. The storage and computation resource is exponentially reduced on the key parameter of holding time, as the qubit number and the circuit depth are both optimized via our compressed state preparation method. The desired information, including the path-dependent and history-sensitive information that is essential for finance and many other practical problems, can be extracted efficiently from the compressed sampling path, and admits a further quadratic speed-up. Moreover, this extraction method is more sensitive to those discontinuous jumps capturing extreme market events. Two applications of option pricing in Merton jump diffusion model and ruin probability computing in collective risk model are given.

I. INTRODUCTION

Continuous time stochastic process (CTSP), encompassing many well known stochastic processes from *Poisson point process*, *compound Poisson process*, *Lévy process*, *continuous Markov process*, to doubly stochastic *Cox process*, is an essential and fundamental mathematical instrument to model and analyse the stochastic world defined on continuous time variables, and it can be applied to a wide range of fields including but not limited to finance, physics, statistics, and biology [1–5]. However, CTSP is usually believed more complicated than its discrete counterpart, due to its continuous paths. On the one hand, for most practical cases of interest, there is no analytic solution or explicit formula to the underlying stochastic differential equation and quantities. On the other hand, since the space of the sampling paths grows exponentially as the time slice goes thinner, unexpectedly large storage and computation resources are consumed when applying numerical methods such as Monte-Carlo simulation [6, 7].

To search for solutions to those difficulties mentioned above, quantum computer would be one powerful tool. Recent developments [8–10] have revealed that quantum computation has great potentiality beyond classical computers. In spite of plenty of algorithms proposed and claimed to have quantum advantage over their classical counterparts [11–17], there are still two essential challenges to overcome when implementing the storage and analysis of CTSP with a quantum computer.

The first challenge is to efficiently encode and prepare the desired CTSP: As being a common and primary bottleneck faced by quantum machine learning and many other quantum algorithms[18], the state preparation problem has been studied and discussed in many works [19–21]. A quantum analogue simulators is proposed to predict the future of a renewal process with less information about the past, and a (perhaps) unbounded reduction in the memory requirement is made in [22], and the quantum advantage in simulating stochastic process is further discussed in [23]. Nevertheless, the CTSP preparation problem have not been totally solved by those works, since they are restricted to the preparation of renewal process and the memory improvements provided by quantum dynamics, respectively. While the storage of historical information is absent, leading crucial practical problems for path-dependent Monte-Carlo simulation, financial time series analysis, quantitative trading, and many other applications.

Besides state preparation, the second challenging problem is the information extraction of CTSP. Quantum Monte-Carlo simulation, which means to generate random paths and compute the expectation of desired value, has been proven to admit a quadratic quantum speed up on computing the final value of discrete paths [24–29], and a weightless summation of discrete paths aiming on Asian-type option pricing is proposed [26], while the expectation of a weighted integral on CTSP paths and the extraction of history-sensitive information (such as first-hitting time) are left unsolved.

In this work, a framework is established to solve the problems of preparation and information of quantum continuous time stochastic process (QCTSP). Encoding method with two representations for general CTSP is introduced and the corresponding state preparation

* wuyuchun@ustc.edu.cn

† gpguo@ustc.edu.cn

method is developed to prepare the CTSP with less qubit number requirement, higher flexibility, and more sensitivity to discontinuous jumps that are important to model extreme market events such as *flash crash*. An observation is made on the CTSP holding time, inducing further reductions on the circuit depth and the gate complexity. Specific quantum circuits are designed for most of the often-used CTSPs with exponential reduction of both qubit number and circuit depth on the key parameter of QCTSP named holding time τ_{avg} (as summarized in table II). As for the information extraction problem of QCTSP, by computing the summation of directed areas, the weightless integral and the arbitrary time weighted integral of the QCTSP can be efficiently evaluated. This enables the quantum Monte-Carlo framework to extend to the continuous-time regime, admitting a quadratic quantum speed up. Moreover, by introducing a sequence of flag qubits, our method can extract the history-sensitive information that is essential and indispensable for quantitative finance, path-dependent option pricing and actuarial science, to cite but a few examples.

Applications of computing the European type option price under the *Merton Jump Diffusion* model and the time value of ruin in a *Collective Risk Model* are given. The first application of valuating a European type option has been studied in previous work [25–27, 29], while our method takes the more practical situation of the discontinuous price movement into consideration and the simulation result is consisted with the *Merton* formula. The second application of computing the ruin probability opens up new opportunities in the area of insurance as being the first time that quantum computing is introduced into insurance mathematics up to known, illustrating the great potential power in CTSP analysis.

In addition to the theoretical importance and rich applicability of QCTSP mentioned above, our work also benefits from its low requirement on input data and circuit connectivity: It can be utilized as an input without quantum random access memory (qRAM) [30–32], partly solving the input problem that quantum machine learning and many other quantum algorithms are confronted with. Simultaneously, a statistics is given in this work to characterize not only the preparation procedure’s complexity but the circuit connectivity as well.

The structure of this article is as follows: Given the mathematical notations in table I for readability and the formal statement of our encoding method at the beginning of section II, the main results of state preparation and information extraction are organized in subsection II A, subsection II B and subsection II C, respectively. Followed by two applications of option pricing and insurance mathematics in section III, the discussion together with an introduction of future work is given in section IV. The detailed construction of specific modified subcircuits and proofs can be found in the APPENDIX.

TABLE I. Mathematical Symbols

Notation	Nomenclature
\mathbb{P}	The probability.
Ω	Space of CTSP
$\tilde{\Omega}_n$	Space of CTSP of n deterministic pieces
\mathcal{S}	Space of states of point
S	the size of the Space of states $S = \mathcal{S} $
\mathbb{Z}_S	The set of index $\{1, \dots, S\}$
T	Time slices
\mathbb{Z}_T	The set of time $\{1, \dots, T\}$
n	Number of Pieces
$X(t)$	A CTSP
X_j	The j^{th} piece’s value variable
x_{j,k_j}	A realization of X_j , taking the $k_j \in \mathcal{S}$ index, in path
Y_j	The j^{th} piece’s increment
τ_j	The j^{th} piece’s holding time
t_j	A realization of τ_j in path
T_j	The j^{th} piece’s cumulative time
$\mathcal{ML}(X)$	The memory length of $X(t)$

II. RESULTS

Framework. In general, for a given CTSP, the most significant distinction from the discrete case is the uncountable dimensional space of continuous sample paths. As the time slices become thinner, the sample space turns out to be a disaster for both theoretical analysis and simulation. In subsection II A, the time compression encoding method that records the piece-wise deterministic space state and its holding time as a discrete pair is introduced instead of the uniform sampling method. And this method benefits from the reduction of qubit number (as shown in Fig. 2), as well as the ability to capture randomly happened discontinuous jumps (as circled in Fig. 4 (a) and Fig. 6 (a)). Two equivalent representations are proposed simultaneously on the purpose of efficiently computing path-dependent and history-sensitive information as stated later.

Although this compressed encoding method appears to be natural and simple, leading a reduction on qubit number and circuit depth, there are still prominent challenges to overcome when we try to prepare a CTSP through this way: By introduction of the statistics *memory length*, and the observation of memory-less process’ holding time, the circuit depth of specific types of process can be further reduced. The basic idea and the detailed construction are both given in subsection II B. In brief, both the qubit number and the circuit depth are determined by the number of pieces n and the average holding time τ_{avg} . The qubit number can be reduced from $O(T \ln S) = O(n\tau_{avg} \ln S)$ of the uniform sampling method to $O(n \ln(\tau_{avg} S))$ of the QCTSP method, making an exponential reduction on the parameter τ_{avg} . And the circuit depth can be optimized from $O(T \ln nS) = O(n\tau_{avg} \ln(nS\tau_{avg}))$ of the uniform sampling method to $O(n \ln(nS))$ of the QCTSP method, also making an exponential reduction of qubit number on the parameter

τ_{avg} .

One even more challenging problem discussed in subsection II C is the corresponding decoding and information extraction method so that the quantum speedup on preparation will not be diminished. By a controlled rotation gate-based Riemann summation of rectangles, the weightless summation of discrete path can be extended to the time integral of continuous path. In addition, a coordinate transformation can be implemented parallel to achieve a path-dependent weighted integral. Furthermore, benefited from our encoding and extracting method, the discontinuous jumps and transitions can be detected and modeled more precisely. And history-sensitive information such as first hitting time can be extracted easily as a consequence. Moreover, by introducing the amplitude estimation algorithm, the information extraction QCTSP also admits a further quadratic speed-up.

A. Compressed Encoding Method

Formally speaking, given the mathematical symbols in table I, and a discrete state space or its discretization $\mathcal{S} (S = |\mathcal{S}| \in \mathbb{N}_+)$, a CTSP can be defined as:

Definition 1. (Continuous Time Stochastic Process) Given a discrete space \mathcal{S} , A continuous time stochastic process $\{X(t) : t \geq 0\}$ is a stochastic process defined on the continuous variable t where for each t_0 , the state $X(t_0) \in \mathcal{S}$ is a stochastic variable whose possibility distribution is determined by $\mathbb{P}[X(t_0)] = \mathbb{P}[X(t_0)|X(t) : 0 \leq t < t_0]$.

The uncountable dimensional space of continuous sample paths is denoted by Ω , and the reduced space $\bar{\Omega}_n$ consists of those paths that can be divided into finite $n \in \mathbb{N}_+$ in-variate pieces. Each $\{X(t) : t \geq 0\}$ in $\bar{\Omega}_n$ is therefore a piece-wise determined random function $X(t) = X_j$ for $T_{j-1} \leq t < T_j$ with $T_0 = 0$. Thus the j^{th} piece can be recorded as a pair of random variables (X_j, τ_j) , where $X_j \in \mathcal{S}$ is a discrete random variable that denotes the j^{th} piece's state, and $\tau_j = T_j - T_{j-1} \in \mathbb{N}^+$ is a strictly positive random variable that denotes the length of lifetime of the j^{th} piece. In this way, the whole CTSP is encoded via a sequence of random variable pairs $\{(X_j, \tau_j) : 1 \leq j \leq n\}$, which will be called the *holding time representation* hereafter (as illustrated in FIG. 1 (a)). More precisely, one have:

Definition 2. (Holding Time Representation of Quantum Continuous Time Stochastic Process) Given a continuous time stochastic process $\{X(t) : t \geq 0\}$, the holding time representation of quantum continuous time stochastic process is a sequence of stochastic pairs (X_j, τ_j) satisfies: (1) $X(t) = X_j : T_{j-1} \leq t < T_j$, (2) $\tau_j = T_j - T_{j-1}$, and (3) $\mathbb{P}[X_j, \tau_j] = \mathbb{P}[X_j, \tau_j | X_{j'}, \tau_{j'} : 1 \leq j' < j]$.

An alternative method named *increment representation* to encode a CTSP is to consider an equivalent sequence of random variable pairs $\{(Y_j, T_j) : 1 \leq j \leq n\}$ where $Y_1 = X_1$ and $Y_j = X_j - X_{j-1}$ are the increments of the CTSP (as illustrated in FIG. 1 (b)):

Definition 3. (Increment Representation of Quantum Continuous Time Stochastic Process) Given a continuous time stochastic process $\{X(t) : t \geq 0\}$, the increment representation of quantum continuous time stochastic process is a sequence of stochastic pairs (Y_j, T_j) satisfies: (1) $X(t) = X_j : T_{j-1} \leq t < T_j$, (2) $Y_j = X_j - X_{j-1}$, and (3) $\mathbb{P}[Y_j, T_j] = \mathbb{P}[Y_j, T_j | Y_{j'}, T_{j'} : 1 \leq j' < j]$.

As the CTSP and the embedded discrete stochastic pairs both lie in the probability space, the notation of specific realizations are needed for the computation of the path probability: A realization of the embedded sequence (X_1, \dots, X_n) and its corresponding index vector are denoted by two vectors $\mathbf{x} = (x_{1,k_1}, \dots, x_{n,k_n})^T \in \mathcal{S}^n$ and $\mathbf{k} = (k_1, \dots, k_n)^T \in \mathbb{Z}_{|\mathcal{S}|}^n$, where $x_{j,k_j} = x(k_j) : 1 \leq j \leq n, 1 \leq k_j \leq |\mathcal{S}|$ means that the j^{th} piece takes the k_j^{th} value in space \mathcal{S} . Meanwhile, a realization of the sequence (τ_1, \dots, τ_n) is represented by the vector $\mathbf{t} = (t_1, \dots, t_n)^T \in \mathbb{Z}_T^n$ where $1 \leq t_j \leq T$ means that the j^{th} piece stays for t_j time slices truncated by T .

For the most general case, the CTSP can be stored by introducing three registers named index register, data register and time register for the storage of the index sequence $\{k_j\}$, the path sequence $\{X_j\}$ and the holding time sequence $\{\tau_j\}$, respectively. The qubit number is reduced from $O(T)$ to $O(n)$ (As illustrated in FIG. 2). Then the QCTSP state lying in the Hilbert space $\mathcal{H}_{k,x} \otimes \mathcal{H}_t = (\mathbb{Z}_{|\mathcal{S}|} \mathbb{C} \mathbb{Z}_{|T|})^{\otimes n}$ can be represented as

$$\begin{aligned} |\psi_f\rangle &= \sum_{\mathbf{k}, \mathbf{t} \in \mathbb{Z}_{|\mathcal{S}|}^n \otimes \mathbb{Z}_T^n} p(\mathbf{k}, \mathbf{t}) |\mathbf{k}\rangle U(\mathbf{k}) |\psi\rangle \otimes |\mathbf{t}\rangle \\ &= \sum_{\mathbf{k}, \mathbf{t} \in \mathbb{Z}_{|\mathcal{S}|}^n \otimes \mathbb{Z}_T^n} p(\mathbf{k}, \mathbf{t}) |\mathbf{k}, \mathbf{x}(\mathbf{k})\rangle \otimes |\mathbf{t}\rangle, \end{aligned} \quad (1)$$

where the unitary operator $U() : \mathbb{Z}_{|\mathcal{S}|}^n \times \mathbb{Z}_T^n \rightarrow \mathcal{B}(\mathcal{H}_k \otimes \mathcal{H}_x \otimes \mathcal{H}_t)$ maps a $2n$ -length vector \mathbf{k}, \mathbf{t} to a linear operator on $\mathcal{H}_k \otimes \mathcal{H}_x \otimes \mathcal{H}_t$. And the possibility amplitudes satisfy $\sum_{\mathbf{k}, \mathbf{t}} p^2(\mathbf{k}, \mathbf{t}) = 1$. For each time piece, the current pair (X_j, τ_j) is derived from the past pieces $\{(X_{j'}, \tau_{j'}) : 1 \leq j' \leq j-1\}$ with the possibility amplitude $p(\mathbf{k}, \mathbf{t})$ satisfies

$$\begin{aligned} p(\mathbf{k}, \mathbf{t}) &= p(X_1 = x(k_1)) \\ &\quad \times p(\tau_1 = t_1 | X_1 = x(k_1)) \\ &\quad \times \prod_{j=2}^n p(X_j = x(k_j) | X_{j'}, \tau_{j'} = x(k_{j'}), t_{j'} : 1 \leq j' < j) \\ &\quad \times \prod_{j=2}^n p(\tau_j = t_j | X_{j'}, \tau_{j'} = x(k_{j'}), t_{j'} : 1 \leq j' < j \\ &\quad \text{and } X_j = x(k_j)). \end{aligned} \quad (2)$$

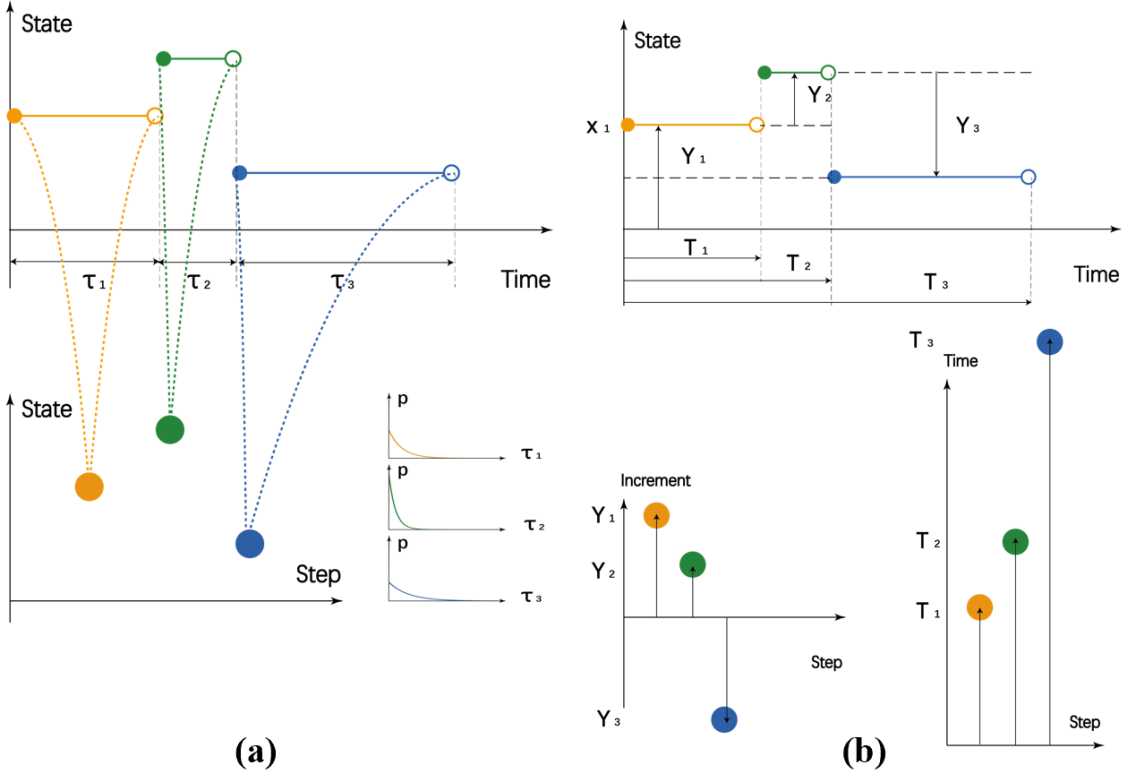


FIG. 1. **Embed a Continuous Time Stochastic Process to a pair of Discrete Stochastic Processes.** In this figure, a continuous time stochastic process is embedded into discrete stochastic processes via two different representations. **(a)** As shown in the left subfigure, the j^{th} in-variant piece of CTSP can be compressed into a discrete random variable X_j (denoted by the point) in the state space, together with a holding time variable τ_j follows a given probability distribution (illustrated by a picture of the probability density function). **(b)** As shown in the right subfigure, the j^{th} in-variant piece of CTSP can be compressed into a discrete random variable of increment $Y_j = X_j - X_{j-1}$ (denoted by the vertical arrow) in the state space, together with an ending time variable T_j (denoted by the horizontal arrow).

Hence the present pair registers (X_j, τ_j) should be entangled with all past time pairs of variables $\{(X_{j'}, \tau_{j'}) : 1 \leq j' \leq j-1\}$ together (as illustrated in FIG. 3 (a)), and this surely leads to a disaster of circuit depth and gate complexity.

B. Efficient State Preparation Method

To see why the state preparation procedure of QCTSP is non-trivial, it should be noticed that the sequence of pairs (X_j, τ_j) can be entangled with each other for $1 \leq j \leq n$. Intuitively, the more the current state is influenced by the past information, the more complicated gates and deeper circuits are needed. More precisely, the memory length of a given CTSP is defined as

$$\begin{aligned} \mathcal{ML}(X(t)) = \min \{n | \mathbb{P}[X(t_0)|X(t) : 0 \leq t < t_0] = \\ \mathbb{P}[X(t_0)|X(t) : t_0 - n\Delta t \leq t < t_0] \\ \text{for all } t_0 \geq n\Delta t\}, \end{aligned} \quad (3)$$

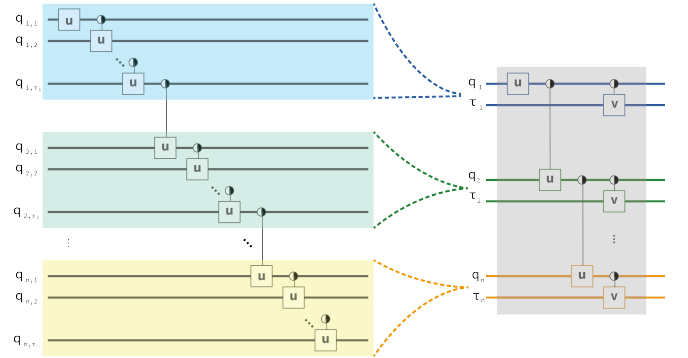


FIG. 2. **Embed a Continuous Time Stochastic Process to a pair of Discrete Stochastic Processes.** In this figure, a continuous time stochastic process is embedded into a sequence of stochastic pairs. Both the qubit number and the circuit depth is reduced as shown.

which means that the conditional probability distribution of current the time t_0 is totally determined by the information in the latest $\mathcal{ML}(X)$ time slices. Two extreme situations are compared in Fig. 3: One is the worst case

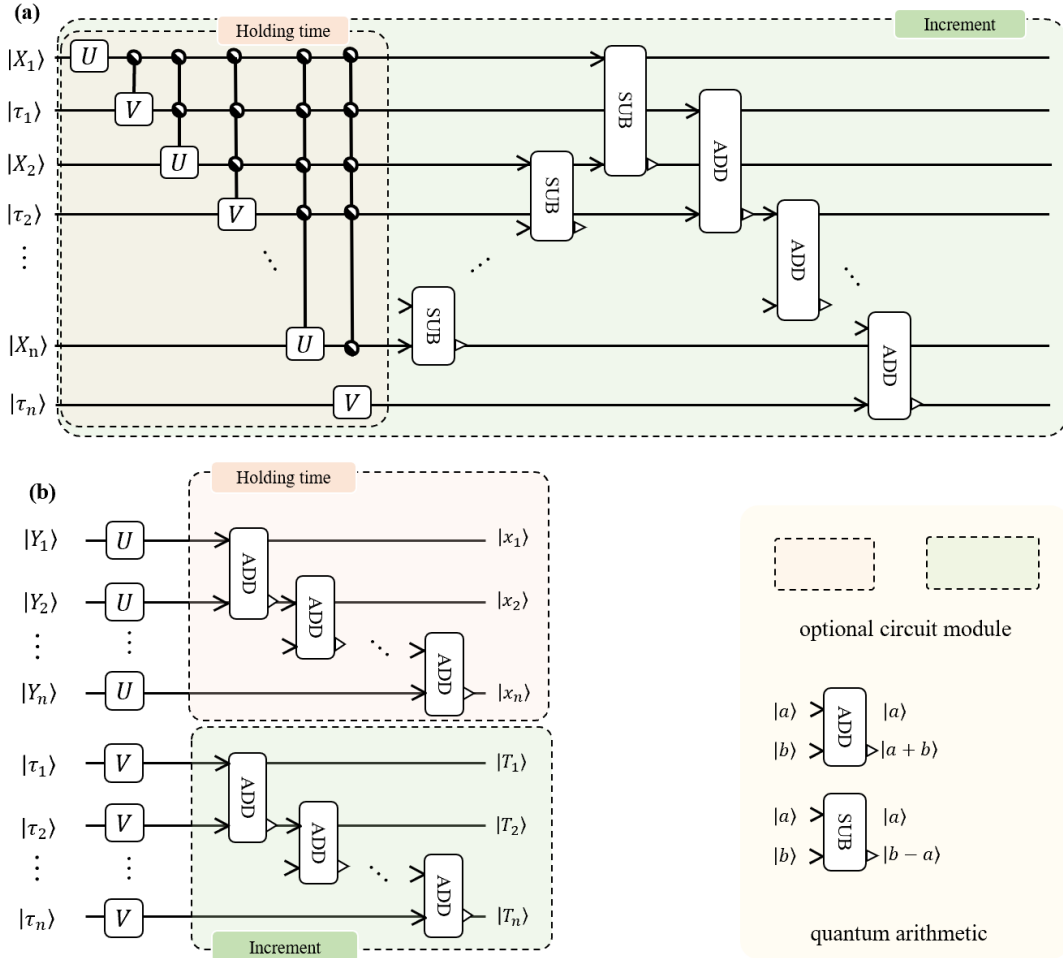


FIG. 3. **Quantum Circuits for General CTSP and compound Poisson Process** In this figure, QCTSPs of $\mathcal{ML}(X) = n$ and *compound Poisson process* of $\mathcal{ML}(X) = n$ are given for comparison. (a) The preparation circuit of the general CTSP is shown and the qubits storing X_j and τ_j are highly entangled. Even for the most simple case where $\mathcal{S} = \{0, 1\}$ and $T = 2$, the circuit are too complicated to efficiently simulated. For the j^{th} step, there are 2^{2j-2} U_j operators and 2^{2j-1} V_j operators, and hence the total number of unitary operators turns to be $2^{2n} - 1$ and increases exponentially. Besides, the growth of the operator size leads to enormous challenges of gate decomposition and long-term entanglement. (b) The preparation of the Poisson process and compound Poisson process is shown. The increments Y_j and holding time τ_j are I.I.D and can be prepared parallel through U and V operators. The alternative encoding methods can be evaluated through a sequence of add operators on Y_j and τ_j registers in the two boxes, with respect to holding time representation and increment representation.

where the memory length $\mathcal{ML}(X) = n$ is as long as the number of pieces, the other is the opposite case where the memory length $\mathcal{ML}(X) = 0$, and in this case $X(t)$ is said to be memory-less. While the first case of general QCTSP preparation procedure has been proved to be complicated in the previous subsection II A, the second case, on the contrary, turns to be quite simple and we have the following result:

Theorem 1. (Memory-less Process' Holding Time) *Supposing that $\{X(t) : 0 \leq t \leq T\}$ is memory-less, then the holding time τ_j for any state X_j follows an exponential distribution $\mathbb{P}[\tau_j \geq t] = e^{-\lambda_j t}$ with λ_j determined by the current state X_j . Moreover, given an ϵ such that the cumulative density function(c.d.f) f sat-*

isfies $\mathbb{P}[\tau_j > T] = 1 - f(T) = e^{-\lambda_j T} < \epsilon$, τ_j can be prepared via a circuit consisting of $\lceil \log(-\frac{1}{\lambda_j} \ln \epsilon) \rceil$ qubits with constant circuit depth 1, and the gate complexity is $\lceil \log(-\frac{1}{\lambda_j} \ln \epsilon) \rceil$. (see proof in Appendix B 1)

This simple result should not be surprising since, as discussed above, the memory-less condition $\mathcal{ML}(\tau_j) = 0$ leads to no-entanglement states and easier preparation. Following this thought, most of the often-used CTSPs have been systematically studied and efficiently prepared. The conclusion that the complexity of the state preparation of QCTSP tends to be higher as the memory length grows is further evidenced by those results summarized in table II, leaving the detailed explanation and relevant applications given as follows.

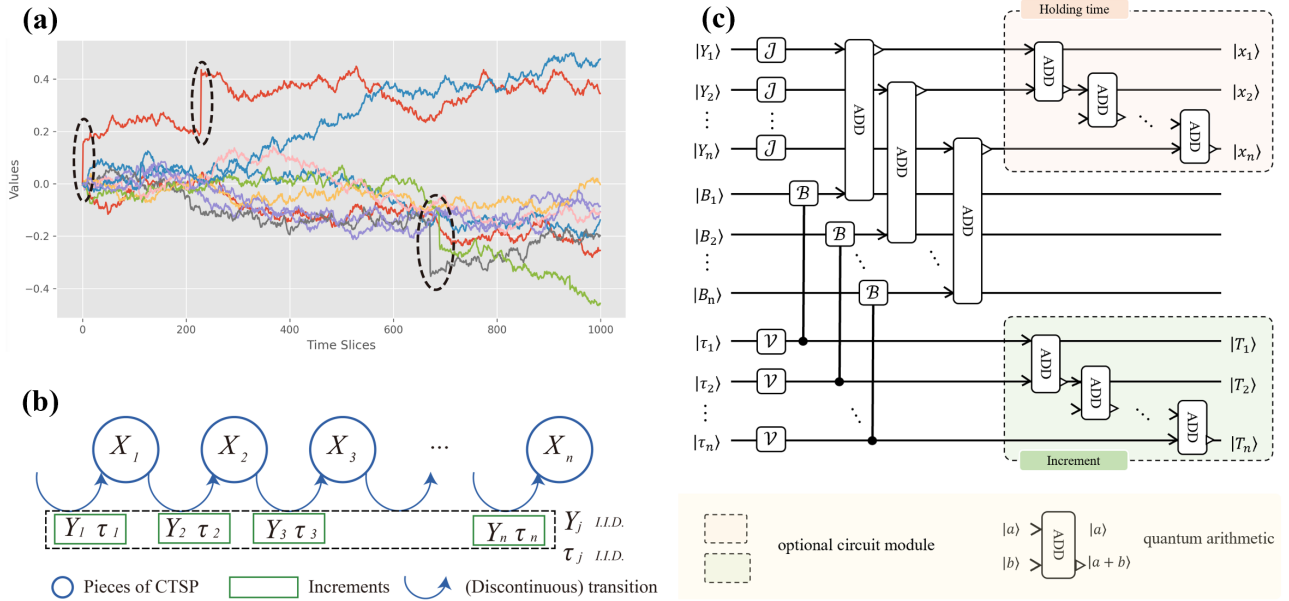


FIG. 4. **Prepare a Lévy Process.** In this figure, the preparation of a general Lévy Process is given: (a) 10 simulated Lévy process paths of 1000 steps: The intensity of discontinuous jump is $\lambda = 1$, and the standard deviation of jump size is $v = 0.3$. The standard deviation and the drift rate of the Brownian part are $\sigma = 0.2$ and $a = 0.02$, respectively. As circled in the picture, discontinuous jumps happen at random timestamps that are hard for a uniform sampling method to capture. (b) A Lévy Process is embedded into discrete stochastic processes via holding time representation and increment representation encoding methods. As $\mathcal{ML}(X) = 0$, the corresponding stochastic pairs (Y_j, τ_j) are I.I.D. variables. (c) The preparation of the general Lévy process is shown. The discontinuous jumps J_j and holding times τ_j are I.I.D and can be prepared parallel through J and V operators. The Brownian motion components B_j are determined by the holding time τ_j , and can be derived by parallel controlled- B operators. The increments $Y_j = J_j + B_j$ are then computed by parallel adder operators. It should be mentioned that operators in the grey box are implemented parallel within constant circuit depth. The alternative encoding methods can be evaluated through a sequence of adder operators on Y_j and τ_j registers in the two boxes, with respect to holding time representation and increment representation.

Lévy Process. The first and essential family of CTSPs is the Lévy process, which is one of the most well-known family of continuous-time stochastic processes, including the Poisson process and the Wiener process (also known as Brownian motion), with applications in various fields. Formally, $\{X(t) : t \geq 0\}$ is said to be a Lévy process if 1) the increments $\{X(T_{j+1}) - X(T_j) : 1 \leq j \leq n\}$ are independent for any $0 < T_1 \leq T_2 \leq \dots \leq T_n$, and 2) stationary which means that $X(t) - X(s)$ depends only on $t - s$ and hence is equal in distribution to $X(t - s)$ (as illustrated in FIG. 4 (a) and (b)). Under these assumptions, a Lévy process for the most general case can be prepared efficiently, and we have the following result:

Theorem 2. (Upper bound of general Lévy Process' preparation) *Supposing that $\{X(t) : 0 < t < T\}$ is a Lévy process, Δt is the length of step, $n = \frac{T}{\Delta t}$ is the length of sample path, and $S = |\mathcal{F}|$ is the number of discretization intervals of the underlying distribution \mathcal{F} . Then the Lévy process can be prepared on $n \log(nS)$ qubits within $O(S + n \log(nS))$ circuit depth, and the gate complexity is thus $O(n(S + \log(nS)))$. (see proof in Appendix B 2)*

It should be mentioned that the preparation procedure's complexity is mainly determined by two factors:

the sampling times $n = \frac{T}{\Delta t}$ and the preparation complexity of the underlying distribution \mathcal{F} . In the most general case where compensated generalized Poisson process with countably many small jump discontinuities and Wiener process are taken into consideration, the sample space size $S = |\mathcal{F}|$ is large and the preparation procedure of the underlying distribution \mathcal{F} may consume enormous resource of classical computation. Hence it is requisite for one to study the more specific situations besides the upper bound given in Theorem 2, and some optimized preparation results are given below. The first example is the that plays an essential role modeling the arrival of independent random events. More precisely, despite several equivalent definitions towards different domains and applications, a CTSP is a *Poisson point process* on the positive half-line if the increment Y_j is a constant 1 and the underlying distribution of each holding time τ_j between the events is an exponential distribution that can be prepared efficiently as shown in Theorem 1. As a direct consequence, one have:

Corollary 3. (Poisson Point Process' preparation) *Supposing that $\{X(t) : 0 < t < T\}$ is a Poisson process, Δt is the length of step, $n = \frac{T}{\Delta t}$ is the length of*

sampling times, and ϵ is the truncation of the exponential distribution $\mathcal{F}(\lambda)$. Then the Poisson process can be prepared on $n\lceil\log(-\frac{n\ln\epsilon}{\lambda})\rceil$ qubits with $O(n\lceil\log(-\frac{n\ln\epsilon}{\lambda})\rceil)$ control-rotation gates, and the circuit depth is $\lceil\log n\rceil$. (see proof in Appendix B 3)

Another more flexible example is the *compound Poisson process* as a generalization, i.e., the jumps' random arriving time follows a Poisson process and the size of the jumps is also random with a underlying distribution \mathcal{G} . Noticed that the each point's sampling space size S of *compound Poisson process* is usually fixed in practical, apparently different from the general Lévy process discussed above, one get the following result with some modification on the circuit(as illustrated in FIG. 3 (b)):

Corollary 4. (Compound Poisson Process' preparation) Suppose that $\{X(t) : 0 < t < T\}$ is a compound Poisson process with $n = \frac{T}{\Delta t}$ being the length of sample path, S denoting the sampling space size of each point, and ϵ being the truncation of the exponential distribution $\mathcal{F}(\lambda)$, then the compound Poisson process can be prepared on $n\lceil\log(-\frac{nS\ln\epsilon}{\lambda})\rceil$ qubits. The circuit depth is $S + n\lceil\log(nS)\rceil$, and the gate complexity is $O(n\lceil\log(-\frac{nS\ln\epsilon}{\lambda})\rceil)$. (see proof in Appendix B 3)

According to the Lévy-Itô decomposition, a general Lévy process can be decomposed into three components: a Brownian motion with drift $\sigma B_t + at$, a compound Poisson process Y_t , and a compensated generalized Poisson process Z_t as follows:

$$X_t = \sigma B_t + at + Y_t + Z_t, \quad (4)$$

where σ is the volatility of the Brownian motion, a is the rate of drift, Y_t is the compound Poisson process of jumps larger than 1 in absolute value, and Z_t is a pure jump process with countably (infinite) many small jump discontinuities. As Z_t contains infinitely many jumps as a zero-mean martingale, it is hard and unnecessary for preparation, and one can prepare a general Lévy process without compensated parts as follows: Firstly, the sequence of exponential jumps J_j and holding times τ_j are prepared via \mathcal{J} and \mathcal{V} operators, respectively. Secondly, the Brownian motions B_j are derived by Grover's state preparation method through \mathcal{B} operators controlled by holding time τ_j . Thirdly, an adder operator is introduced for the sum of pure jump and Brownian parts. It should be mentioned that the drift term at has been omitted since any function on this linear term can be easily translated into a function and hence well-evaluated by Theorem 7 and Theorem 8. The total circuit is shown in FIG. 4 (c).

Continuous Markov Process. The second and more complicated family of CTSPs is the *continuous Markov process*. In brief, a stochastic process is called a *continuous Markov process* if it satisfies the Markov condition: For all $t \geq 0$, $s \geq 0$, $\mathbb{P}[X(s+t) = j|X(s) = k \wedge X(u) : 0 \leq u < s] = \mathbb{P}[X(s+t) = j|X(s) = k]$, where

$j, k \in \mathcal{S}$. Intuitively speaking, given the present state $X(s)$, the future $\{X(s+t) : t \geq 0\}$ is independent of the passed history $\{X(u) : 0 \leq u < s\}$, and the memory length of a *continuous Markov process* is $\mathcal{ML}(X_t) = 1$ (shown in FIG. 5 (a) and (b)). A *continuous Markov process* can be efficiently prepared mainly for two reasons: the holding time τ_j only depends on the current state X_j , while the state sequence $\{X_j\}$ is independent from $\{X_{j'} : 1 \leq j' < j - 1\}$. As a result, the *continuous Markov process* can be embedded into an independent discrete Markov chain that depicts the transition of different states, together with a sequence of exponential distributions circuits, which carry the information of the holding time, controlled by it (as illustrated in FIG. 5 (c)). More precisely, we have the following result:

Theorem 5. (Continuous Markov Process' Preparation) Supposing a stochastic process $\{X(t) : t \geq 0\}$ with discrete state space $\mathcal{S} \subseteq \mathbb{Z}$ to be a continuous-time Markov chain. Then it can be prepared on $n\lceil\log(-\frac{S}{\lambda_{min}} \ln \epsilon)\rceil$ qubits via a quantum circuit consisting of $O(nS\lceil S + \log(-\frac{\ln \epsilon}{\lambda_{min}})\rceil)$ gates and nS^2 circuit depth, where $S = |\mathcal{S}|$, λ_{min} is the minimum of λ_j , and ϵ is the truncation error bound for time. (see proof in Appendix B 4)

Cox Process. As a further evidence illustrating the flexibility and generalizability of our encoding method, the Cox process, a useful framework for modeling prices of financial instruments in financial mathematics [33], can be efficiently prepared. It is one of the most significant distinctions between Cox process and those processes discussed above that both the states and the evolution law vary randomly over time (as illustrated in FIG. 6 (a) and (b)). As a direct consequence, the preparation procedure and the corresponding circuit should be dynamic and flexible to characterize this doubly stochastic property (shown in FIG. 6 (c)). Precisely speaking, a Cox process is a generalization of Poisson process where the intensity $\lambda(t)$ itself is also a stochastic variable of some distribution \mathcal{F} . The preparation procedure can be divided into two steps: Firstly, the stochastic control sequence of λ_j is prepared by some F operator for the underlying distribution \mathcal{W} . And secondly, the holding time sequence τ_j is prepared by parallel controlled- V operators for the underlying exponential distribution. The operators of different exponential distributions can be implemented by a sequence of controlled-rotation gates of different rotation angles. The increments Y_j are assumed to be I.I.D. and can be prepared through some G operators (normal choice of distributions can be found in appendix, see FIG. 15(a) and FIG. 15(c) for reference). In summary, we have the following result:

Theorem 6. (Cox Process' Preparation) Suppose that $\{X(t) : t \geq 0\}$ is a Cox process with varying intensity variable $\lambda(t)$, and $\lambda(t)$ follows an underlying statistics distribution \mathcal{F} that can be prepared on $q_{\mathcal{F}}$ qubits with

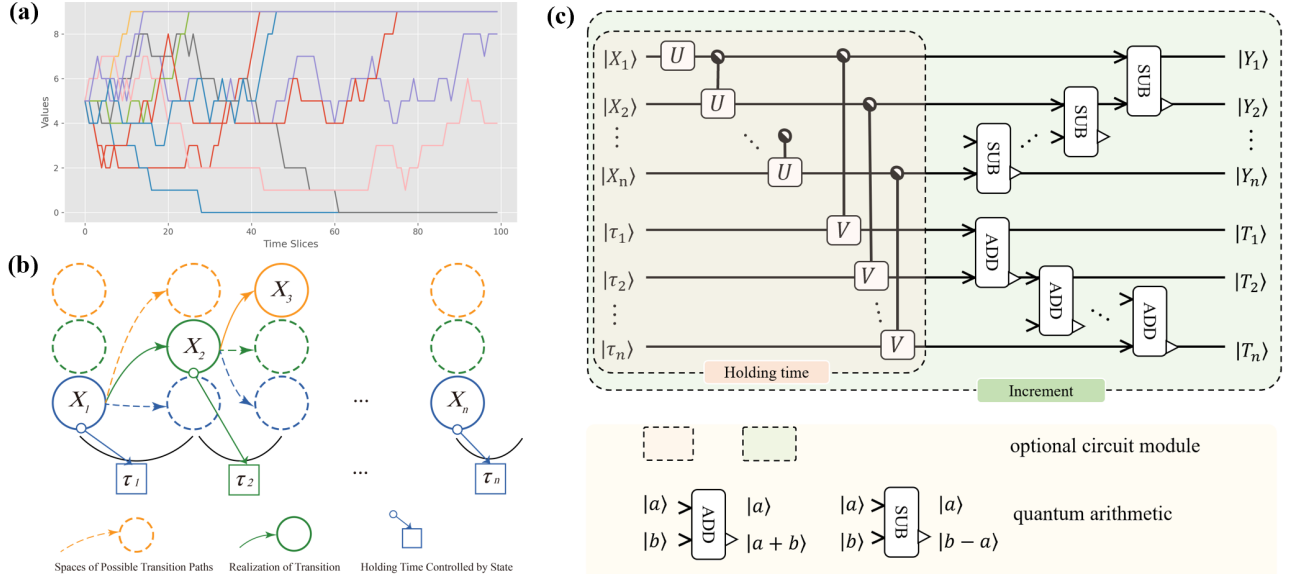


FIG. 5. Prepare a Continuous Markov Process. In this figure, the preparation of a continuous Markov Process is given: **(a)** 10 simulated *continuous Markov process* paths of 100 steps: The transition rates from $|n\rangle$ to $|n-1\rangle$ and $|n+1\rangle$ are both 0.05, and the state $|0\rangle$ and $|10\rangle$ are absorbing states. Since the possibility to stay in the current state is $p = 0.9$, the continuous Markov process tends to be in-variant for long holding time, and thus it can be compressed a lot via our encoding method. **(b)** The *continuous Markov process* is embedded via both holding time representation and increment representation. Due to $\mathcal{ML}(X) = 1$, each piece's state space X_j is controlled by the previous one X_{j-1} while the holding time τ_j is determined by the current state X_j through an exponential distribution. **(c)** The preparation procedure of a *continuous Markov process* is shown. The embedded discrete Markov process X_j is prepared by a sequence of U and controlled- U operators, while the holding time τ_j is then determined by X_j and prepared by controlled- V operators. The increment representation is then prepared by an alternative sequences of adder and subtractor subcircuits in the box.

circuit depth $d_{\mathcal{F}}$. The increments Y_j follows an *I.I.D.* that can be prepared on q_G qubits with circuit depth d_G . Also it is supposed that the minimum value of $\lambda(t)$ is λ_{min} and the error bound is ϵ , then it can be efficiently prepared on $O(n(q_{\mathcal{F}} + q_G - \frac{\ln \epsilon}{|\lambda|_{min}})))$ qubits with circuit depth $O(\max\{q_G, q_{\mathcal{F}} + 2^{d_{\mathcal{F}}}\} + nq_G)$ (holding time representation) or $O(\max\{q_G, q_{\mathcal{F}} + 2^{d_{\mathcal{F}}}\} - \frac{n \ln \epsilon}{\lambda_{min}})$ (increment representation). (see proof in Appendix B 5)

As the details of the preparation procedure of a QCTSP have been given in the above theorems, the results are summarized in table II. From a high level view, the computation and storage resource of the preparation procedure is totally determined by the time length T and the memory length $\mathcal{ML}(X)$ of the underlying QCTSP $X(t)$. By our compressed encoding method and the corresponding preparation procedure, the number of the copies of the state space is reduced from $O(T) = O(n\tau_{avg})$ of the uniform sampling method to $O(n \ln \tau_{avg})$ of the QCTSP method, leading an exponential reduction of qubit number on the parameter τ_{avg} . By the encoding method and the observation on the holding time of the memory-less QCTSP, the circuit depths can be optimized from $O(T \ln nS) = O(n\tau_{avg} \ln(nS\tau_{avg}))$ of the uniform sampling method to $O(n \ln(nS))$ of the QCTSP method, also making an exponential reduction of qubit number on the parameter τ_{avg} .

C. Information Extraction Method

Besides the state preparation problem, another challenge of QCTSP is to decode the compressed process and rebuild the information of interest. To extract desired information from QCTSP, instead of the discrete summation $\mathbb{E}[f(S_n)] = \sum_{\mathbf{j} \in K^n} f(\text{sum}\{\mathbf{x}(\mathbf{j})\})\mathbb{P}[\mathbf{X} = \mathbf{x}(\mathbf{j})]$ as studied in [29], one needs to evaluate its continuous counterpart, i.e., the integral of random variable X on time t .

Weightless Integral. More specifically, the expectation value of an integrable function $f : \mathbb{R} \rightarrow \mathbb{R}$ of the random variable

$$I(X, T) = \int_{t=0}^T X(t) dt \quad (5)$$

can be efficiently evaluated via a framework developed as follows: First of all, the integral can be divided into vertical boxes (as shown in FIG. 7 (a)) as a Riemann summation

$$I(X, T) = \int_{t=0}^T X(t) dt = \sum_{j=0}^n X_j \tau_j.$$

Secondly, the area Z_j of each box is translated into a multiplication on the holding time representation encoding

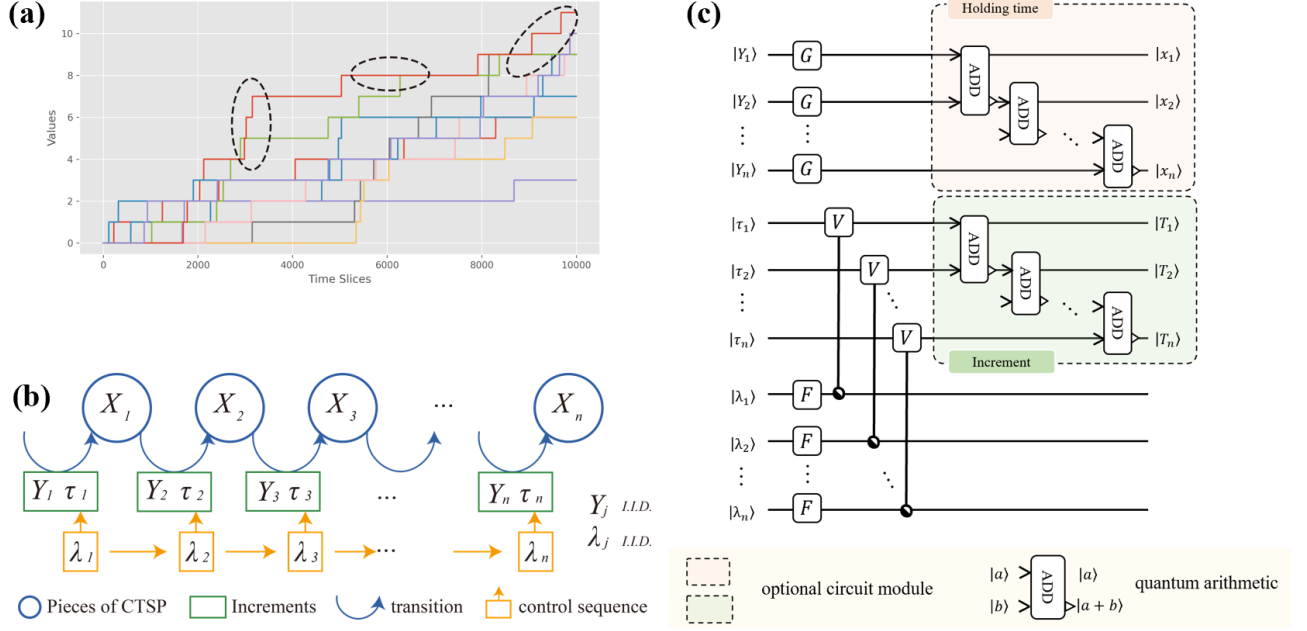


FIG. 6. **Prepare a Cox Process.** In this figure, the preparation of a continuous Markov Process is given: **(a)** 10 simulated Cox process paths of length 10 and 10000 steps: The varying intensity follows an exponential distribution with $\lambda = 0.1$, and the size of the discontinuous jump is assumed to be a constant 1. As circled in the picture, the intensity changes with time and the jump rate varies from high to low randomly. **(b)** A Cox Process is again embedded via holding time representation and increment representation encoding methods. The process is more complicated as the holding time Y_j of interest is controlled by another stochastic variable λ_j and the increment Y_j and the control variable λ_j are independent identical distribution variables, respectively. **(c)** The preparation of a Cox process is shown. Firstly, the stochastic control sequence λ_j is prepared by F operators, and then the holding time sequence τ_j is prepared by parallel controlled- V operators. The increments Y_j are I.I.D. and can be prepared through G operators. Alternative subcircuits of holding time and increment representations follow as shown in the two boxes.

variables X_j and τ_j . Benefited by the encoding method, this expression turns to be quite simple (as illustrated in FIG. 7 (c)). Thirdly, the expected value of the integrable function $f(\sum_{j=0}^n X_j \tau_j)$ can be evaluated through a Fourier approximation $f_{P,L}(x) = \sum_{l=-L}^L c_l e^{i \frac{2\pi l}{p} x}$ as a P -periodic function of order L :

$$\sum_{l=-L}^L c_l (\mathbb{E}[\cos(\frac{2\pi l}{p} (\sum_{j=1}^n Z_j))] + i \mathbb{E}[\sin(\frac{2\pi l}{p} (\sum_{j=0}^n Z_j))]).$$

Each term $\mathbb{E}[\cos(\frac{2\pi l}{p} (\sum_{j=0}^n Z_j))]$ and $\mathbb{E}[\sin(\frac{2\pi l}{p} (\sum_{j=0}^n Z_j))]$ can be evaluated via rotation gates on the target qubit controlled by Z_j followed by a standard amplitude estimation algorithm. Leaving the detailed proof in the appendix, one have:

Theorem 7. (Evaluating $I(t)$) Suppose that a QCTSP $\{X(t) : t \geq 0\}$ is given via holding time representation with n steps, l_x, l_τ qubits for each pair X_j, τ_j , and \mathcal{P} circuit depth. And also one have that $f_{P,L}(x)$ is the P -periodic L -order Fourier approximation of the desired integrable function of the random variable $f : \mathbb{R} \rightarrow \mathbb{R}$. Then given the error ϵ , the expectation value of $f(I(X, T)) = f(\int_{t=0}^T X(t) dt)$ can be efficiently evaluated within $O(\mathcal{P} + nl_x l_\tau)$ circuit depth and

$O(\frac{LP}{\epsilon}(\mathcal{P} + nl_x l_\tau))$ time complexity. (see proof in Appendix C1)

Weighted Integral. Moreover, this framework applies to the more complicated and generalized situation where the time structure is taken into consideration and thus has no discrete correspondence. Introducing a time-dependent function $g(t)$, we can evaluate the expectation value of an integrable function $f : \mathbb{R} \rightarrow \mathbb{R}$ of the random variable

$$J(X, T) = \int_{t=0}^T g(t) X(t) dt. \quad (6)$$

Since the time structure $g(t)$ is taken into consideration, the integral is divided into horizontal directed boxes (as shown in FIG. 7 (b)):

$$J(X, T) = \sum_{j'=1}^n Y_{j'} (\sum_{j=j'}^n G_j) = \sum_{j=1}^n W_j.$$

Due to a trade-off on circuit depth and qubits number (see FIG. 7 (d) and FIG. 7 (e) for reference), this summation can be evaluated via either holding time representation

or increment representation. Similiar Fourier approximation and amplitude estimation are employed to compute

$$\sum_{l=-L}^L c_l (\mathbb{E}[\cos(\frac{2\pi l}{p}(\sum_{j=1}^n W_j))] + i\mathbb{E}[\sin(\frac{2\pi l}{p}(\sum_{j=0}^n W_j))]),$$

and hence the following result is given:

Theorem 8. (Evaluating $J(t)$) *i) Suppose that a QCTSP $\{X(t) : t \geq 0\}$ is given via holding time representation with n steps, l_x, l_τ qubits for each pair X_j, τ_j , and \mathcal{P} circuit depth. $g(t)$ is a function whose integral can be efficiently prepared with \mathcal{F} circuit depth. And also one have that $f_{P,L}(x)$ is the P -periodic L -order Fourier approximation of the desired integrable function of the random variable $f : \mathbb{R} \rightarrow \mathbb{R}$. Then given the error ϵ , the expectation value of $f(J(X, T)) = f(\int_{t=0}^T g(t)X(t) dt)$ can be efficiently evaluated within $\mathcal{P} + \mathcal{F} + nl_x l_\tau + n \max(l_x, l_\tau)$ circuit depth and $O(\frac{LP}{\epsilon}(\mathcal{P} + \mathcal{F} + nl_x l_\tau + n \max(l_x, l_\tau)))$ time complexity.*

ii) Suppose that a QCTSP $\{X(t) : t \geq 0\}$ is given via increment representation with n steps, l_Y, l_T qubits for each pair Y_j, T_j , and \mathcal{P} circuit depth. $g(t)$ is a function whose integral can be efficiently prepared with \mathcal{G} circuit depth. And also one have that $f_{P,L}(x)$ is the P -periodic L -order Fourier approximation of the desired integrable function of the random variable $f : \mathbb{R} \rightarrow \mathbb{R}$. Then given the error ϵ , the expectation value of $f(J(X, T)) = f(\int_{t=0}^T g(t)X(t) dt)$ can be efficiently evaluated within $O(\mathcal{P} + \mathcal{G} + nl_Y l_T)$ circuit depth and $O(\frac{LP}{\epsilon}(\mathcal{P} + \mathcal{G} + nl_Y l_T))$ time complexity. (see proof in Appendix C2)

Therefore our algorithms would enable the quantum Monte-Carlo method to apply to path-dependent and continuous stochastic processes, including the time weighted expectation of random variables $\mathbb{E}[f(\frac{1}{T} \int_{t=0}^T tX(t) dt)]$, and the exponential decay time weighted expectation of random variables $\mathbb{E}[f(\int_{t=0}^T e^{-\alpha t} X(t) dt)]$ that are usually used in mathematical finance and quantitative trading.

history-sensitive information. Besides those global information defined on the whole path studied above, there is another category of history-sensitive problem that plays an essential role in statistics and finance, including first passage time of Brownian motion, surviving time of ruin theory, and survival analysis, to name but a few. The most apparent difference of the first-hitting problem is that the path-dependent information need to be extracted knowing the whole history path, and can not be derived directly by a quantum walk (as illustrated in Fig. 8). Formally, a first-hitting problem can be regarded as evaluating the following

$$K(X, T, B) = \inf \{t : X(t) > B | 0 < t < T\}. \quad (7)$$

The basic idea to evaluate Eq.(7) is to consider n flag qubits storing the comparison result of each piece in the sampling path. As a discontinuous jump representing extreme events or market hits always happens at the end of a piece, this method shall work much more precisely than the uniform sampling method. Formally speaking, supposing a given bound B , to derive the first hitting time, a bound information register and a flag register is introduced with $O(\log B)$ and n qubits, respectively. For the j^{th} piece of QCTSP, the remained value is derived through a controlled subtraction whose control qubit is F_{j-1} and carry-out qubit is F_j . And a CNOT gate is implemented to flip the F_j qubit controlled by the F_{j-1} qubit. For each piece, two classes are distinguished: Before the first hit, the remained bound is $\sum_{j'=1}^{j-1} Y_{j'} \leq B$, and the flag register is $\underbrace{|1\dots 10\dots 0\rangle}_{j-1} flag$. This first class

can be divided into two cases: If the hit does not happen at the j^{th} piece, the state of the carry-out qubit F_j after the subtraction remains $|0\rangle$, and then is flipped by the CNOT gate. Hence one have:

case 1 ($\sum_{j'=1}^{j-1} Y_{j'} \leq B$ and $\sum_{j'=1}^j Y_{j'} < B$):

$$\begin{aligned} & |B - \sum_{j'=1}^{j-1} Y_{j'}\rangle_{bound} \underbrace{|1\dots 10\dots 0\rangle}_{j-1} flag \\ \xrightarrow{\text{controlled}} & |B - \sum_{j'=1}^j Y_{j'}\rangle_{bound} \underbrace{|1\dots 10\dots 0\rangle}_{j-1} flag \\ \xrightarrow{\text{CNOT}} & |B - \sum_{j'=1}^j Y_{j'}\rangle_{bound} \underbrace{|1\dots 10\dots 0\rangle}_j flag. \end{aligned}$$

If the hit happens at the j^{th} piece, the state of the carry-out qubit F_j after the subtraction turns to be $|1\rangle$, and then is flipped by the CNOT gate. Hence one have:

case 2 ($\sum_{j'=1}^{j-1} Y_{j'} \leq B$ and $\sum_{j'=1}^j Y_{j'} > B$):

$$\begin{aligned} & |B - \sum_{j'=1}^{j-1} Y_{j'}\rangle_{bound} \underbrace{|1\dots 10\dots 0\rangle}_{j-1} flag \\ \xrightarrow{\text{controlled}} & |B - \sum_{j'=1}^j Y_{j'}\rangle_{bound} \underbrace{|1\dots 10\dots 0\rangle}_j flag \\ \xrightarrow{\text{CNOT}} & |B - \sum_{j'=1}^j Y_{j'}\rangle_{bound} \underbrace{|1\dots 10\dots 0\rangle}_{j-1} flag \end{aligned}$$

For the second class where the current piece is after the first hit $\sum_{j'=1}^{j''} Y_{j'} > B$, the flag register is $\underbrace{|1\dots 10\dots 0\rangle}_{j''} flag$, and the subtraction and CNOT gates will not be implemented, and thus the result is:

case 3 ($\sum_{j'=1}^{j''} Y_{j'} > B$ for some $j'' < j$):

$$\begin{aligned} & |B - \sum_{j'=1}^{j''} Y_{j'}\rangle_{\text{bound}} \underbrace{|11\dots10\dots0\rangle}_{j''-1} \text{flag} \\ \xrightarrow[\text{subtractor}]{\text{controlled}} & |B - \sum_{j'=1}^{j''} Y_{j'}\rangle_{\text{bound}} \underbrace{|11\dots10\dots0\rangle}_{j''-1} \text{flag} \\ \xrightarrow{\text{CNOT}} & |B - \sum_{j'=1}^{j''} Y_{j'}\rangle_{\text{bound}} \underbrace{|11\dots10\dots0\rangle}_{j''-1} \text{flag} \end{aligned}$$

Leaving the theoretical analysis as future work, examples of option pricing and ruin theory will be given in the next section as proof of principle.

III. APPLICATIONS

In this section, two applications of QCTSP in different financial scenes are given to illustrate the wide range of applicability of QCTSP. In subsection III A, the first application is focused on the option pricing problem where the underlying stock price is no longer continuous Brownian motion and the original *Black-Scholes* formula fails. By simulation of QCTSP, option pricing is solved in a different way from previous works and is consisted with the more practical *Merton Jump Diffusion* formula. In subsection III B, the problem of computing the ruin probability under the *Collective Risk Model* is studied, introducing quantum algorithm into the field of insurance mathematics.

A. European Option Pricing under the Merton Jump Diffusion Model

Since firstly being introduced into the field of financial engineering, CTSP has been proven to be a powerful tool for financial derivatives pricing [34, 35]. Among those financial derivatives, the European call option is one basic instrument that gives someone the right to buy an underlying stock S_T by a given knock price K at the fixed maturity time T . The famous *Black-Scholes* model is proposed to value a European option [36], and the simulation for *Black-Scholes* type option pricing has been implemented on quantum computers [25–27, 29]. However, the assumption of a constant variance log-normal distribution in the original article [36] turns to be less realistic as the empirical studies of discontinuous returns of stock are ignored. Hence the *Merton Jump diffusion* model was proposed to incorporate more realistic assumptions by Merton's work [37].

In the *Merton Jump diffusion* model, the stock price S_T is assumed to satisfy the following stochastic differ-

ential equation:

$$\begin{aligned} \ln S_T = \ln S_0 & + \int_{t=0}^T (r - \frac{\sigma^2}{2} - \lambda(m + \frac{v^2}{2})) dt \\ & + \int_{t=0}^T \sigma dW(t) \\ & + \sum_{j=1}^{Poi(T)} (J_j - 1), \end{aligned} \quad (8)$$

where S_0 is the current stock price, T is the maturity time in years, r is the annual risk-less interest rate, σ is the annual volatility, $dW(t)$ is the Weiner process, $Poi(T)$ is the *Poisson point process*, and J_j is the j^{th} discontinuous jump follows a log-normally distribution. The last term on the right hand side represents the discontinuous price movements caused by such as acquisitions, mergers, corporate scandals, and fat-finger errors. A closed form solution $MJD(S, K, T, r, \sigma, m, v, \lambda)$ to Eq.(8) is derived by Merton as an infinite summation of *Black-Scholes* formula $BS(S, K, T, r_j, \sigma_j)$ conditional on the number of the jumps and the underlying distributions of each jump:

$$MJD(S, K, T, r, \sigma, m, v, \lambda) = \sum_{j=0}^{\infty} BS(S, K, T, r_j, \sigma_j), \quad (9)$$

where m is the mean of the jump size, v is the volatility of the jump size, λ is the intensity of the underlying *Poisson point process*, and $r_j = r - \lambda(m - 1) + \frac{j \ln m}{T}$ and $\sigma_j = \sqrt{\sigma^2 + j \frac{v^2}{T}}$ are the corresponding interest rate and volatility, respectively.

In spite of being in line with empirical studies of market returns, the formula Eq. (9) takes the form of an infinite summation, and thus an alternative numerical method of Monte-Carlo can be employed to compute the desired option price. Instead of a Brownian motion in the *Black-Scholes* model, one have to simulate, in the *Merton Jump diffusion* model, the more complicated case of a Lévy process where our method can be applied to make a quadratic speedup against the classical Monte-Carlo simulation. More precisely, for an European type call option, its price given the underlying stock price S_T can be defined as:

$$\begin{aligned} \text{price} & = \max\{S_0 e^{D+B_T+\sum_{j=1}^{Poi(T)} J_j} - K, 0\} \\ & = S_0 e^{\max\{D+B_T+\sum_{j=1}^{Poi(T)} J_j, \ln \frac{K}{S_0}\}} - K, \end{aligned} \quad (10)$$

where $D = (r - \frac{\sigma^2}{2} - \lambda(m + \frac{v^2}{2}))T$ is the adjusted drift term on the purpose of risk neutral preferences, B_T represents the Brownian motion term and follows a normal distribution $N(0, \sigma\sqrt{T})$, and J_j represents the j^{th} discontinuous jump and follows a normal distribution $N(m, v)$.

This Lévy process can be efficiently prepared as mentioned in subsection II A, and then the valuation procedure is implemented via the method given in subsection II C. More specifically, the quantum circuit, as illustrated

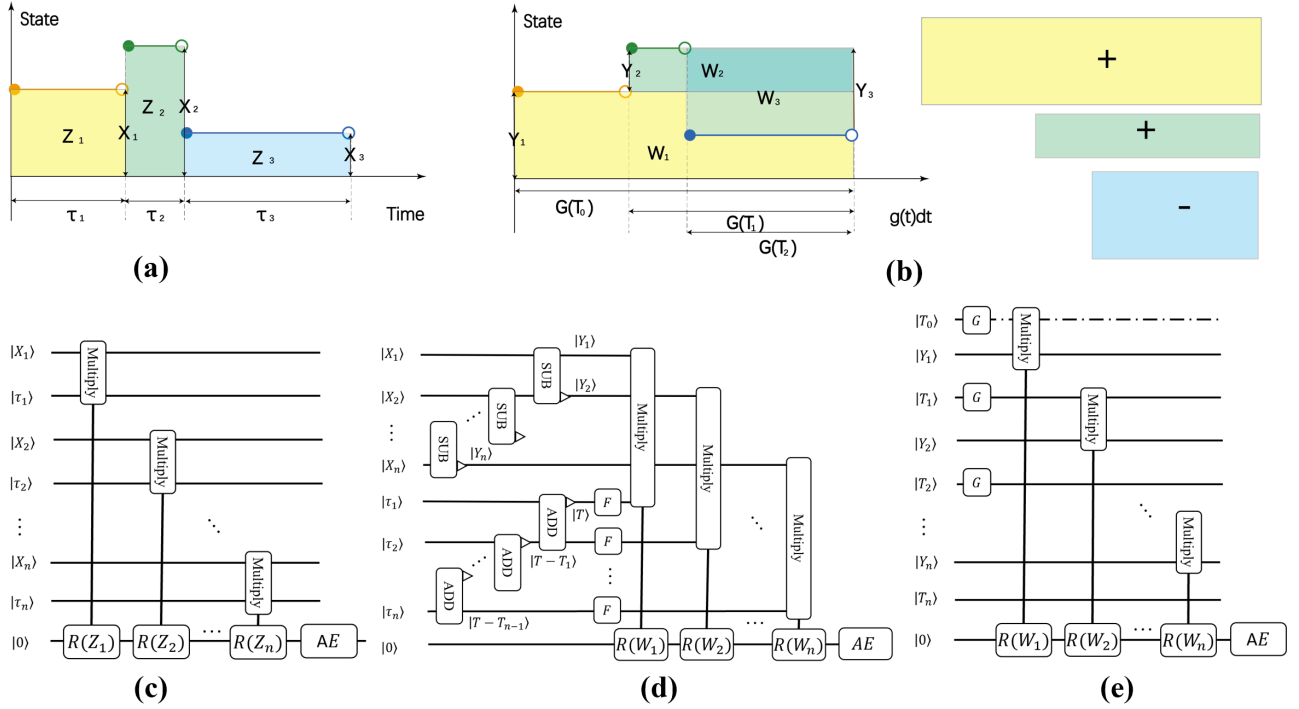


FIG. 7. Information Extraction for Quantum Continuous Time Stochastic Process. (a) The integral $I(X, T) = \int_{t=0}^T X(t) dt$ is represented as a summation of area of rectangles derived from vertical division $I = \sum Z_j$. (b) By a coordinate transformation $t \rightarrow g(t)$, the integral $J(X, T) = \int_{t=0}^T g(t)X(t) dt$ can be represented as a summation of directed area of rectangles derived from horizontal division $J = \sum W_j$: the yellow and green boxes both correspond to positive increments $Y_{1,2}$ and area $W_{1,2}$, while the blue box corresponds to a negative increment Y_3 and W_3 . (c) The circuit for the evaluation of $I(t)$ is shown. Supposing that X_j and τ_j have been prepared as the input state, n quantum multipliers are introduced to evaluate $Z_j = X_j\tau_j$: Rotation operators controlled by Z_j are implemented on the target qubit followed by a standard amplitude estimation subcircuit in the red box. (d) The circuit for the evaluation of $J(t)$ for holding time representation is shown. Supposing that X_j and τ_j have been prepared as the input state, then a sequence of subtractor operators is introduced to derive the increments Y_j , and another sequence of adder operators is introduced to evaluate the cumulative time from ending time $T - T_{j-1} = \sum_{j'=j}^n \tau_{j'}$. Hence $\int_{T_{j-1}}^T g(t) dt = F(T - T_{j-1})$ can be evaluated through the integral operators F . Following that are the desired variables $W_j = Y_j F(T - T_{j-1})$ by quantum multiplier operators: Rotation operators controlled by W_j are implemented on the target qubit followed by a standard amplitude estimation subcircuit in the red box. (e) The circuit for the evaluation of $J(t)$ is shown. Supposing that Y_j and T_j have been prepared as the input state, one more qubit is introduced to denote the beginning time T_0 , followed by unitary operators G act on T_j to derive $G(T_{j-1})$. Then a sequence of multiplier operators are implemented to compute the desired product $W_j = Y_j G(T_{j-1})$: Rotation operators controlled by W_j are implemented on the target qubit followed by a standard amplitude estimation subcircuit in the red box. The circuit's depth is less than in subfigure (d) as a consequence of increment representation's advantage on integral calculation.

in Fig. 9, consists of six quantum registers: the maturity time register $|T\rangle$, the holding time register $|\tau_j\rangle$, the flag register $|F_j\rangle$, the jump size register $|B_j\rangle$, the Brownian motion size register $|G\rangle$, and the target qubit $|Target\rangle$. The holding time τ_j can be prepared via parallel exponential distribution subcircuits $\mathcal{J} = Exp(\lambda T)$, and the jump size B_j can be prepared via parallel normal distribution subcircuits $\mathcal{B} = Norm(m, v)$. The drift term together with the geometric Brownian motion is prepared on $|G\rangle$ via a normal distribution subcircuit $\mathcal{D} + \mathcal{B}' = Norm((r - \frac{\sigma^2}{2} - \lambda(m + \frac{v^2}{2}))T, \sigma\sqrt{T})$. Subtractor and controlled-subtractors together with X gate and CNOT gates are implemented to justify the number of jumps that will be taken into consideration, and the

result is output on the flag register $|F_j\rangle$. Adders controlled by the corresponding flag registers are employed to derive the final value of the stock price. A rotation gate is then implemented on the target qubit, controlled by the signed summation on register $|\theta_{sum}\rangle$. Then the final value of the option price can be valued via a measurement or an amplitude estimation.

The corresponding quantum simulation result can be found in Fig. 10 and Fig. 11. In Fig. 10, the underlying stock price is given with $S_0 = 100$, $K = 100$, $r = 0.1$, $\sigma = 0.02$, $T = 1$, and $\Delta t = \frac{1}{30}$, and the range of m and v are 0, 0.1, 0.2, 0.3, 0.4 and 0, 0.05, 0.15, 0.2, 0.25, respectively. Due to the restriction on the qubit number of computing resource, the simulation is divided into two steps: 100 groups of random rotation angles corresponding to

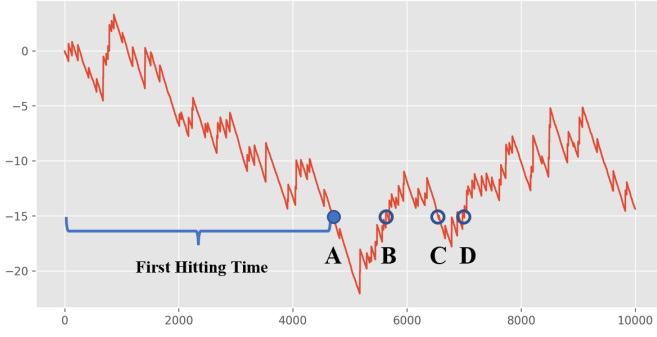


FIG. 8. As shown in this figure, the point **A** represents the first hitting event with the desired first hitting time, while the points **B**, **C**, **D** should not be captured. This information is determined by the knowledge of the whole past path, hence being *history-sensitive*, and can not be extracted by a quantum walk.

the Brownian motion size and jump sizes are generated by classical random generator and then implemented on the target qubit, and 1024 shots of QCTSP simulated paths are repeated for each group. As shown in Fig. 10, the larger the jump size (characterized by m and v) is, the farther the *Merton Jump Diffusion* value is away from the original *Black-Scholes* price as a consequence of the discontinuous jumps. And the QCTSP simulation result is consisted with the 40 terms truncated *Merton Jump Diffusion* formula (Eq. (9)) as well as the classical Monte-Carlo simulation, characterizing the property of Lévy discontinuous jump path well. The robustness of the QCTSP method is illustrated in Fig. 11, where different annual interest rates $r = 0.05, 0.1, 0.15$ are given in the three subfigures with varying jump sizes. As shown in this figure, for a wide range of different parameters, the quantum simulation results are consisted with the Merton Formula.

B. The Time Value Of Ruin

Since being a fundamental means to model the stochastic world, there is no surprise that the QCTSP framework developed in this work has great potential power applied to various fields, including the especially case of ruin theory that plays a central role in insurance mathematics, high-frequency trading's market micro-structure theory, and option pricing [38–41]. In ruin theory, the risk of an insurance company are assumed to be caused by random claims arriving at time $T_j = \sum_{j'=1}^j \tau_{j'}$, wherein the j^{th} claim size ξ_j and inter-claim time τ_j are both assumed to follow independent and identically distributions. Hence the aggregate asset of the insurance company is a continuous time stochastic process

$$X(t) = u + ct - \sum_{j=1}^{Poi(t)} \xi_j, \quad (11)$$

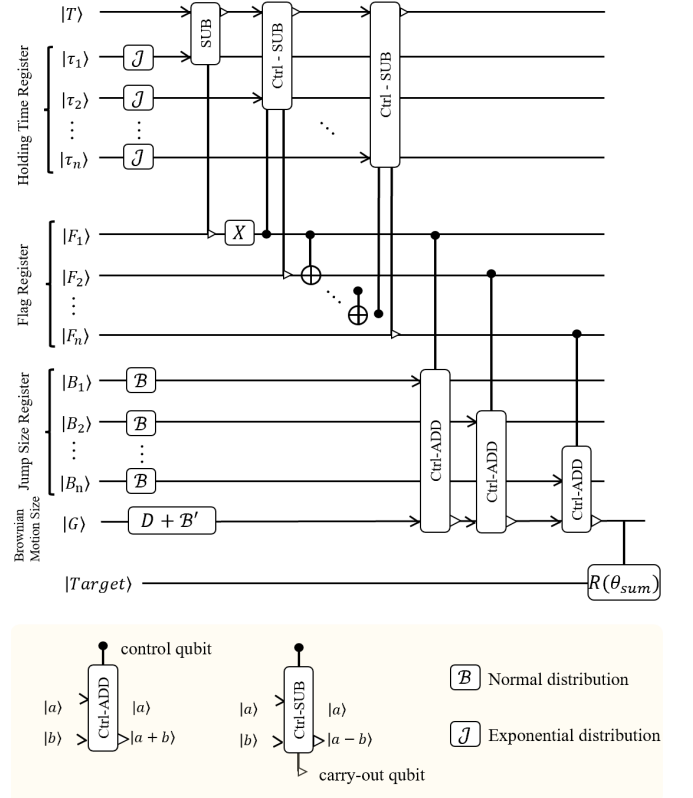


FIG. 9. **QCTSP Circuit of the Simulation of Merton Jump Diffusion Model.** In this figure, the circuit of the simulation of European call option price in *Merton Jump Diffusion* model is presented. The holding time τ_j is prepared via parallel subcircuits $\mathcal{J} = \text{Exp}(\lambda T)$, and the jump size B_j is prepared via subcircuits $\mathcal{B} = \text{Norm}(m, v)$. The drift term together with the geometric Brownian motion is prepared on $|G\rangle$ via the subcircuit $\mathcal{D} + \mathcal{B}' = \text{Norm}((r - \frac{\sigma^2}{2} - \lambda(m + \frac{v^2}{2}))T, \sigma\sqrt{T})$. Subtractor and controlled-subtractors together with X gate and CNOT gates are implemented to justify the number of jumps with output on the flag register $|F_j\rangle$. Adders controlled by the flag registers are employed to derive the final value of the stock price, followed by a rotation gate on the target qubit controlled by the signed summation on register $|\theta_{sum}\rangle$.

where the initial surplus is $X(0) = u$, and the premiums are received at a constant rate c . In the *Collective Risk Model*, also known as the Cramér Lundberg model, the claim number process $Poi(t)$ is assumed to be a Poisson process with intensity λ , and the underlying distribution of τ_j is an exponential distribution. In the Sparre Andersen model, $Poi(t)$ can be extended to a renewal process with arbitrary underlying distribution. Despite of the detailed differences between them, both of the two stochastic processes $X(t)$ in these models are Lévy processes with drift term ct , and hence can be prepared easily via our method.

$$Y(t) = u + ct - X(t) = \sum_{j=1}^{Poi(t)} \xi_j \quad (12)$$

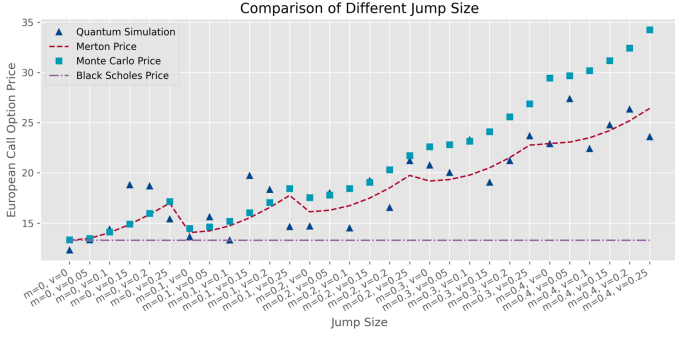


FIG. 10. **Comparison of QCTSP Simulation of European Call Option Price in Merton Jump Diffusion Model with Different Jump Size.** In this figure, the simulation of European call option price in *Merton Jump Diffusion* model is presented. The underlying stock price is given with $S_0 = 100$, $K = 100$, $r = 0.1$, $\sigma = 0.02$, $T = 1$, and $\Delta t = \frac{1}{30}$, and the range of m and v are 0, 0.1, 0.2, 0.3, 0.4 and 0, 0.05, 0.1, 0.15, 0.2, 0.25, respectively. As shown in the figure, the simulated prices are consisted with the Merton formula Eq.(9), and the value is away from the *Black Scholes* formula as the jump size tends to be large.

To go one step further, a great variety of ruin-related quantities fall into the category of the expected discounted penalty function, also known as the time value of ruin, and can be easily derived through a quantum MC modified by us. More precisely, following the notation of Gerber and Shiu [38], the time value of ruin is defined as

$$\phi(u) = \mathbb{E}^{X_t} [e^{-\delta\tau} w(X(\tau-), X(\tau)) \mathbb{I}_{\tau < \infty} | X(0) = u], \quad (13)$$

where $\tau(u) = \inf \{t : U(t) < 0 | U(0) = u\}$ denotes the time of ruin, and $X(\tau-) = u + c\tau - \sum_{j=1}^{N(\tau)-1} X_j$ and $X(\tau) = u + c\tau - \sum_{j=1}^{N(\tau)} X_j$ are the surplus prior to ruin and the deficit at ruin, respectively. The expectation is taken over the probability distribution of the ruin samples, taking an interest discounting factor $e^{-\delta\tau}$ into consideration. The ultimate ruin probability $\psi(u) = \mathbb{P}[X(\tau) < 0 | X(0) = u, \tau < \infty]$ is exactly a special case of Eq.(13) given $\delta = 0$ and $w(x, y) = 1$. Since ruin always happens after a claim,

$$\begin{aligned} \psi(u) &= \mathbb{P}[X(\tau) < 0 | X(0) = u, \tau < \infty] \\ &= \mathbb{E}^{X_t} [\mathbb{I}_{\tau < \infty} | X(0) = u] \\ &= \mathbb{E}^{X_t} [\mathbb{I}_{u + \sum_{j=1}^n (\tau_j - \xi_j) < 0} | n < \infty] \\ &= \mathbb{E}^{Y_t} [\mathbb{I}_{Y(t) < u + ct}], \end{aligned}$$

where the indicator function $\mathbb{I}_{Y(t) < u + ct}$ can be easily derived through a sequence of controlled adder and modified subtractor on the prepared states. The detailed construction of circuits and corresponding simulation result are given in Fig. 12 and Fig. 13.

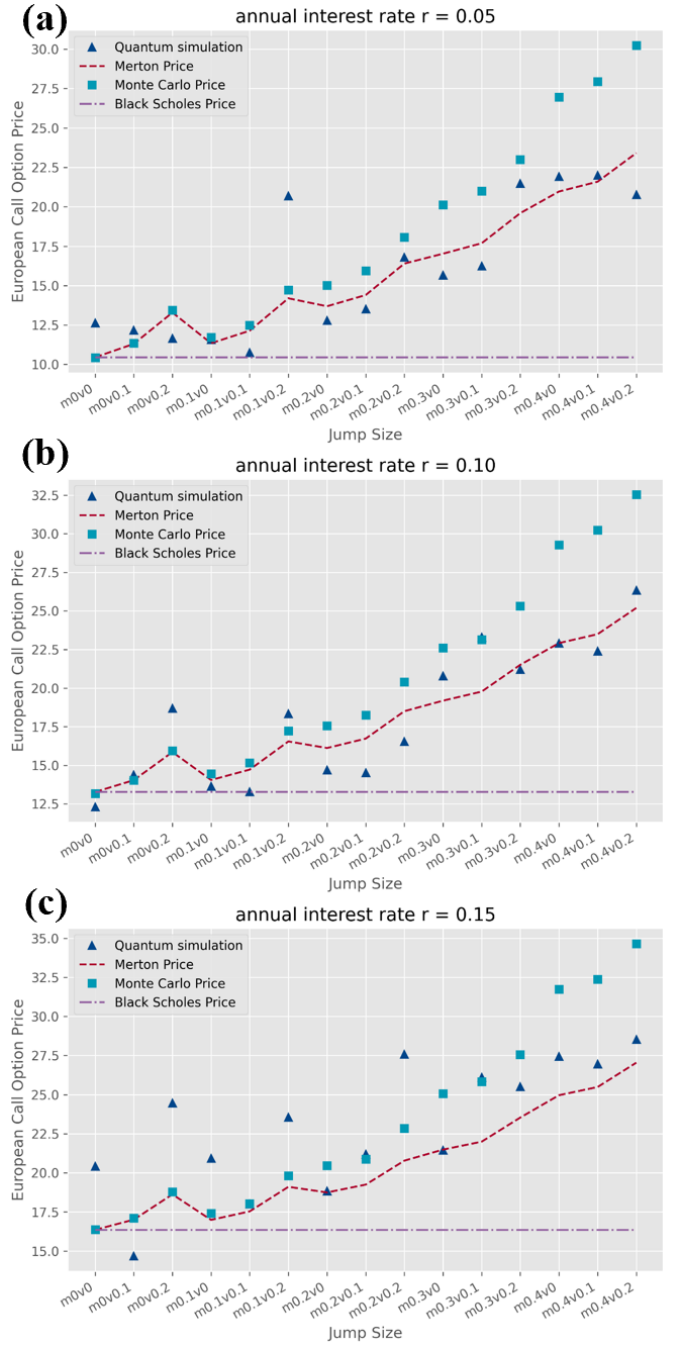


FIG. 11. **Comparison of QCTSP Simulation of European Call Option Price in Merton Jump Diffusion Model with Different Annual Interest.** In this figure, the simulation of European call option price in *Merton Jump Diffusion* model is presented. The underlying stock prices of annual interest rate $r = 0.05, 0.1, 0.15$ are given with $S_0 = 100$, $K = 100$, $\sigma = 0.02$, $T = 1$, and $\Delta t = \frac{1}{30}$, and the range of m and v are 0, 0.1, 0.2, 0.3, 0.4 and 0, 0.1, 0.2, respectively. As shown in the figure, the simulation results are consisted with the Merton formula Eq.(9) while the interest rate, the average jump size, and the volatility of jump size vary, showing robustness with wide ranges of parameters.

TABLE II. **Comparison of QCTSP and Uniform Sampling** In this table, most often-used CTSP's preparation procedure is summarized: the memory length, qubit number and circuit depth of each CTSP type, which have been given in section II B and proved in Appendix B, are listed in the second, third, and fifth columns, respectively.

QCTSP Type	\mathcal{ML}	Qubit Number		Circuit Depth	
		QCTSP (our work)	Uniform Sampling	QCTSP (our work)	Uniform Sampling
Poisson point process	0	$n \lceil \log \left(\frac{-n \ln \epsilon}{\lambda} \right) \rceil$	$\frac{-n \ln \epsilon}{\lambda} \lceil \log \left(\frac{-n \ln \epsilon}{\lambda} \right) \rceil$	$\lceil \log n \rceil$	$\lceil \log \left(\frac{-n \ln \epsilon}{\lambda} \right) \rceil$
compound Poisson process	0	$n \lceil \log \left(\frac{-nS \ln \epsilon}{\lambda} \right) \rceil$	$\frac{-n \ln \epsilon}{\lambda} \lceil \log \left(\frac{-nS \ln \epsilon}{\lambda} \right) \rceil$	$S + n \lceil \log (nS) \rceil$	$S + \frac{-n \ln \epsilon}{\lambda} \lceil \log \left(\frac{-nS \ln \epsilon}{\lambda} \right) \rceil$
Lévy process	0	$n \log (nS')$	$T \log S$	$S' + n \lceil \log (nS') \rceil$	$S + T \log (TS)$
continuous Markov process	1	$n \lceil \log \left(-\frac{S \ln \epsilon}{\lambda_{\min}} \right) \rceil$	$-\frac{n \ln \epsilon}{\lambda_{\min}} \lceil \log \left(-\frac{S \ln \epsilon}{\lambda_{\min}} \right) \rceil$	nS^2	$-\frac{n \ln \epsilon}{\lambda_{\min}} S^2$
k -order Markov process	k	$n \lceil \log \left(-\frac{S \ln \epsilon}{\lambda_{\min}} \right) \rceil$	$-\frac{n \ln \epsilon}{\lambda_{\min}} \lceil \log \left(-\frac{S \ln \epsilon}{\lambda_{\min}} \right) \rceil$	nS^{k+1}	$-\frac{n \ln \epsilon}{\lambda_{\min}} S^{k+1}$
Cox process	0	$n(q_{\mathcal{F}} + q_{\mathcal{G}} - \frac{\ln \epsilon}{ \lambda _{\min}})$	$-\frac{n \ln \epsilon}{ \lambda _{\min}} (q_{\mathcal{F}} + q_{\mathcal{G}})$	$\max \{q_{\mathcal{G}}, q_{\mathcal{F}} + 2^{d_{\mathcal{F}}}\} + nq_{\mathcal{G}}$	$\max \{q_{\mathcal{G}}, q_{\mathcal{F}} + 2^{d_{\mathcal{F}}}\} - \frac{nq_{\mathcal{G}} \ln \epsilon}{ \lambda _{\min}}$
general CTSP	n	$n \log \frac{ST}{n}$	$T \log S$	$\left(\frac{ST}{n}\right)^n$	S^T

IV. DISCUSSION

In our work, the efficient state preparation and quantum-enhanced analysis of continuous time stochastic process are studied. The whole procedure for the preparation of quantum continuous time stochastic process is established: the state can be prepared more sensitive to discontinuous jumps to model the extreme market emergencies while the qubit number and the circuit depth are both reduced exponentially on the key parameter of holding time. Also, new Monte-Carlo simulation method towards QCTSP is proposed. The QCTSP admits a further quadratic speedup against its classical counterpart CTSP, the mainstream instrument in the study of continuous stochastic world. The techniques for the extraction of *weighted integral* and *history-sensitive information*, being essential for quantitative trading, time series analysis, and actuarial mathematics, are developed so that the requirement of extra n copies of random paths, and the implied restriction of I.I.D. condition can both be removed. Two applications on European option pricing under the *Merton Jump Diffusion* model and the ruin probability valuating in *Collective Risk Model* are given as proof of principle.

There are mainly four reasons why QCTSP is one of the proper candidates for practical application in noisy intermediate-scale quantum era. First of all, QCTSP has no input restriction, and can be implemented without assumption of oracle and qRAM. What's more, it can be utilized within *quantum machine learning* and

other quantum algorithms, as a basic subcircuit breaking through the input bottleneck. The second reason is that the QCTSP can be prepared parallel due to a communicative equivalence class decomposition of the sample space, resulting in a qubit number reduction. Thirdly, our QCTSP preparation method makes low requirement on the topological structure of quantum machine: The connectivity requirement concerned with the memory length can be supposed quite low in many situations, and thus most qubits only needs to be entangled with their neighborhood. Lastly, due to the fundamental and critical role CTSP plays in stochastic analysis, the QCTSP is believed to have huge potential for theoretical generalizability and applied flexibility.

In consideration of the conciseness and thematic focus, many interesting applications of QCTSP on different facets such as high-frequency trading, actuarial, and option pricing are left to be solved, too. Besides, more techniques on the efficient extraction of path-dependent information should be studied in the future.

ACKNOWLEDGEMENT

This work was supported by the National Natural Science Foundation of China (Grants No. 12034018), and Innovation Program for Quantum Science and Technology No. 2021ZD0302300.

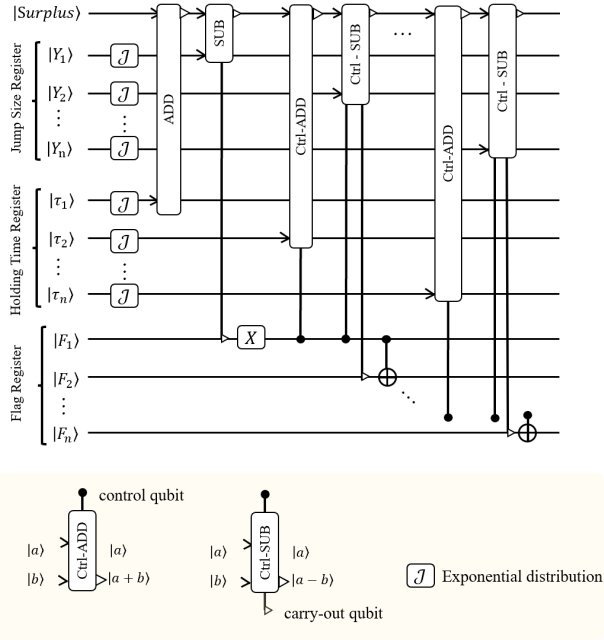


FIG. 12. **Quantum Circuit of Computing Ruin Probability.** The ultimate probability of the *Collective Risk Model* is simulated via this quantum circuit. The receiving rate is assumed to be 1 so that the premium can be summed directly, removing the qubits requirement and the circuit depth from function cT . For each piece of QCTSP, an adder is followed by a controlled-subtractor whose carry-out qubit is on the flag qubit together with a controlled flip, as discussed in subsection III C.

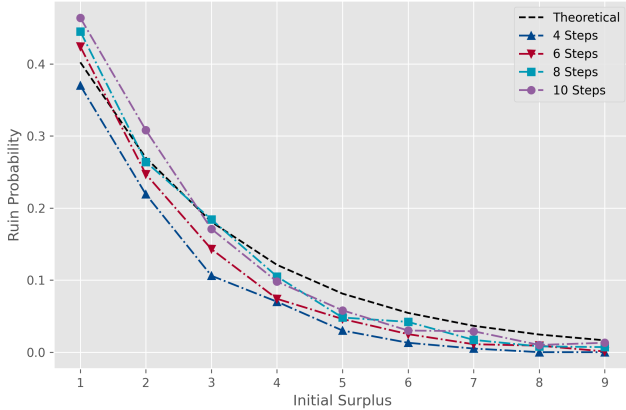


FIG. 13. **Simulation of ultimate ruin probability.** The ultimate probability of the *Collective Risk Model* is simulated for varying initial surplus with sample paths of different lengths. The intensities of inter-claim time and claim size are $\lambda_t = 0.6$, and $\lambda_\xi = 1$, respectively. The sample precision is $\epsilon = 0.001$, and the premiums' receiving rate is $c = 1$. The shot number is set to be 1000 for each simulation point. As shown in the figure, the simulated ruin probabilities of varying surpluses fit the theoretical benchmark well. And the distance from the theoretical curve tends to be smaller as the length of the sample paths grows.

Appendix A: Basic Circuits for Arithmetic and Distribution Preparation

Some basic arithmetic circuits and statistics distribution preparation circuits are given in this appendix.

1. Modified Quantum Subtractor

Although adder and subtractor circuits have been studied in many works (see [42] for reference), some modification is needed in our work as we wish to map $|a\rangle|b\rangle$ to $|a\rangle|a-b\rangle$, i.e., store the result in the second register while leave the first register unchanged. The basic idea is as follows: since $(a' + b)' = a - b$, X gates are introduced to calculate the complement of a as $|a'\rangle|b\rangle$. Then a ripple-carry addition circuit is implemented to output the summation result on the first register $|a' + b\rangle|b\rangle$. Finally, another sequence of X gates are put on the first register $|a - b\rangle|b\rangle$.

2. Quantum Multiplier for Amplitude Estimation and Quantum Monte-Carlo

In this subsection, a quantum multiplier for quantum estimation, and hence quantum Monte-Carlo is given as follows:

Lemma 9. Suppose that $|a\rangle$ and $|b\rangle$ are l_a -bit and l_b -bit strings, respectively, and $|e^{iM\theta_0}\rangle$ is an analog-encoded qubit, then the multiplication of $|a\rangle$ and $|b\rangle$ can be added to $|e^{iM\theta_0}\rangle$ as $|a\rangle|b\rangle|e^{iM\theta_0}\rangle \rightarrow |a\rangle|b\rangle|e^{i(M+ab)\theta_0}\rangle$, within $l_a l_b$ controlled-rotation gates.

Proof. The proof is directly: Given two bit strings $|a\rangle = |x_{l_a} \dots x_2 x_1\rangle$ and $|b\rangle = |y_{l_b} \dots y_2 y_1\rangle$, their product can be computed as

$$\begin{aligned}
 ab &= \left(\sum_{i=1}^{l_a} x_i 2^{i-1}\right) \left(\sum_{j=1}^{l_b} y_j 2^{j-1}\right) \\
 &= \sum_{i=1}^{l_a} \sum_{j=1}^{l_b} x_i y_j 2^{i+j-2}.
 \end{aligned}$$

Hence the term $x_i y_j 2^{i+j-2}$ can be implemented by a rotation gate on the target qubit $|e^{iM\theta_0}\rangle$ controlled by the i^{th} and j^{th} qubits of register $|a\rangle$ and $|b\rangle$, where the rotation angle $\theta_{i,j} = 2^{i+j-2}\theta_0$ is determined by the index i, j only. The final state is:

$$\begin{aligned}
 |e^{iM\theta_0}\rangle &\rightarrow \left|e^{i(M\theta_0 + \sum_{i=1}^{l_a} \sum_{j=1}^{l_b} x_i y_j 2^{i+j-2}\theta_0)}\right\rangle \\
 &= \left|e^{i(M+ab)\theta_0}\right\rangle.
 \end{aligned}$$

If $|a\rangle$ and $|b\rangle$ are signed integers, the rotation gates of two different directions should be controlled by the two sign qubits as well. The total number of controlled rotation gates is $l_a l_b$ as claimed. \square

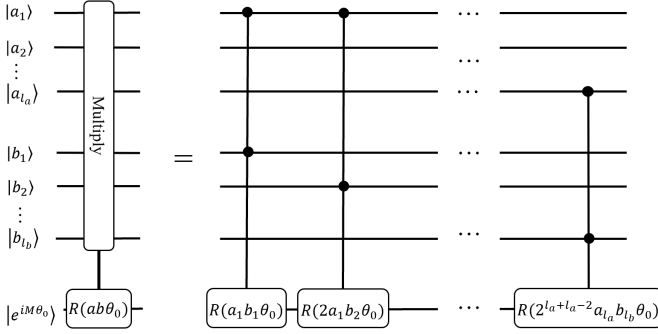


FIG. 14. **Modified Subtractor Circuit.** In this figure, a subtractor circuit of two 3-qubits integers that maps $|a\rangle |b\rangle$ to $|a - b\rangle |b\rangle$ is given. The basic idea is from [42] with some modification so that the result can be stored in the first register leaving the second register unchanged.

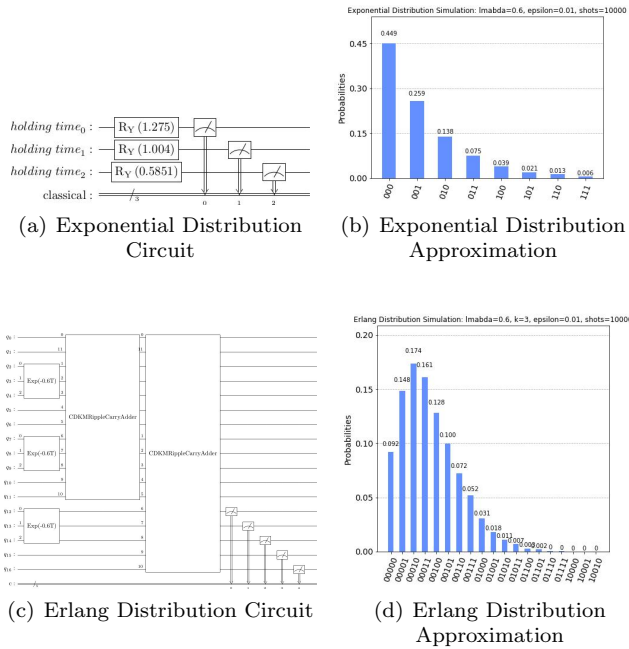


FIG. 15. Preparation of Exponential and Erlang Distribution

3. State preparation for Statistical Distributions

The exponential distribution is implemented by parallel rotation gates as illustrated in FIG. 15(a). Detailed computation of rotation angles is given in Appendix B 1. The Erlang distribution is a summation of several exponential distributions and hence can be prepared via copies of exponential distribution preparation subcircuits together with a sequence of adder operators as shown in FIG. 15(c). Corresponding simulation results are given in FIG. 15(b) and 15(d), respectively.

Appendix B: Proofs for QCTSP State Preparation Problem

1. Proof of Theorem 1

Proof. By the definition of memory-less process, one have

$$\mathbb{P}[\tau_l > s] = \mathbb{P}[\tau_l > t + s | \tau_l > t] = \frac{\mathbb{P}[\tau_l > t + s]}{\mathbb{P}[\tau_l > t]},$$

and hence the c.d.f. $f(t) = \mathbb{P}[\tau_l \leq t]$ satisfies:

$$1 - f(s) = \frac{1 - f(s+t)}{1 - f(t)}.$$

Differentiating with respect to t and setting $t = 0$ leads to

$$\begin{aligned} -f'(s) &= \frac{-f'(s+t)}{1 - f(t)}, \\ -f'(0) &= \frac{-f'(t)}{1 - f(t)}. \end{aligned}$$

Noticing that $-f'(0)$ is a constant, the integrals of the two sides turn to be

$$\begin{aligned} -f'(0)t &= \ln(1 - f(t)) + C \\ f(t) &= 1 - e^{-f'(0)t}, \end{aligned}$$

where the constant C is supposed to be exactly 1 to satisfy $f(\infty) = 1$. Thus the holding time τ_l follows an exponential distribution $\mathbb{P}[\tau_l \geq t] = e^{-\lambda_l t}$ with $\lambda_l = f'(0)$ determined by X_l . As ϵ is given, without loss of generality, T is supposed to be 2^m with $m = \lceil \log(-\frac{1}{\lambda_l} \ln \epsilon) \rceil$ so that

$$T = -\frac{1}{\lambda_l} \ln \tilde{\epsilon} \geq -\frac{1}{\lambda_l} \ln \epsilon, \quad (\text{B1})$$

where

$$\tilde{\epsilon} = e^{-\lambda_l T} < \epsilon \quad (\text{B2})$$

is a more strictly error bound which is easier to compute. On the truncated support set $[0, T)$, simple computation shows that

$$\bar{\mathbb{P}}[t \leq \tau < t+1] = \frac{\mathbb{P}[t \leq \tau < t+1]}{\mathbb{P}[0 \leq \tau < T]} = \frac{e^{-\lambda_l t} - e^{-\lambda_l(t+1)}}{1 - e^{-\lambda_l T}}. \quad (\text{B3})$$

Assuming that the preparation circuit consists of $m = \log T$ qubits initialized to be $|0\rangle$, the j^{th} qubit is then aligned with the rotation gate $R_Y(\theta_j)$ with $\theta_j = \arctan \tilde{\epsilon}^{1/2^{j+1}} : 1 \leq j \leq m$. A direct computation shows

that

$$\begin{aligned}
& \bigotimes_{j=1}^m R_Y(\theta_j) |0\rangle \\
&= \bigotimes_{j=1}^m \left(\frac{1}{\sqrt{1 + \tilde{\epsilon}^{1/2^j}}} |0\rangle + \frac{\tilde{\epsilon}^{1/2^{j+1}}}{\sqrt{1 + \tilde{\epsilon}^{1/2^j}}} |1\rangle \right) \\
&= \bigotimes_{j=1}^m \left(\sum_{k_j=0}^1 \frac{\tilde{\epsilon}^{k_j/2^{j+1}}}{\sqrt{1 + \tilde{\epsilon}^{1/2^j}}} |k_j\rangle \right) \\
&= \sum_{k_1, k_2, \dots, k_m=0}^1 \frac{\tilde{\epsilon}^{\sum_{j=1}^m k_j/2^{j+1}}}{\prod_{j=1}^m \sqrt{1 + \tilde{\epsilon}^{1/2^j}}} |k_1 k_2 \dots k_m\rangle \\
&= \sum_{k_1, k_2, \dots, k_m=0}^1 \sqrt{\frac{1 - \tilde{\epsilon}^{1/2^m}}{1 - \tilde{\epsilon}}} \tilde{\epsilon}^{\sum_{j=1}^m \frac{k_j}{2^{j+1}}} |k_1 k_2 \dots k_m\rangle \\
&= \sum_{k_1, k_2, \dots, k_m=0}^1 \sqrt{\frac{\tilde{\epsilon}^{\sum_{j=1}^m \frac{k_j}{2^j}} - \tilde{\epsilon}^{\frac{1}{2^m} + \sum_{j=1}^m \frac{k_j}{2^j}}}{1 - \tilde{\epsilon}}} |k_1 k_2 \dots k_m\rangle
\end{aligned} \tag{B4}$$

$$= \sum_{t=0}^{T-1} \sqrt{\frac{\tilde{\epsilon}^{\frac{t}{T}} - \tilde{\epsilon}^{\frac{t+1}{T}}}{1 - \tilde{\epsilon}}} |t\rangle \tag{B5}$$

$$= \sum_{t=0}^{T-1} \sqrt{\frac{e^{-\lambda t} - e^{-\lambda(t+1)}}{1 - e^{-\lambda T}}} |t\rangle \tag{B6}$$

$$= \sum_{t=0}^{T-1} \sqrt{\mathbb{P}[t \leq \tau < t+1] |t\rangle} \tag{B7}$$

Here the binary number and the corresponding summation $(k_1 k_2 \dots k_m)_2 = \sum_{j=1}^m k_j 2^{m-j}$ in Eq.(B4) are both substituted by the decimal number t varying from 0 to $T = 2^m$ in Eq.(B5). Then Eq.(B6) and Eq.(B7) are derived by Eq.(B2) and Eq.(B3), respectively. Hence, with $m = \lceil \log(-\frac{1}{\lambda} \ln \epsilon) \rceil$ qubits and the same number of rotation gates, the desired truncated state is successfully prepared (as illustrated in FIG. 15(a) and FIG. 15(b)). \square

2. Proof of Theorem 2

Proof. Given a time interval T , it can be uniformly divided into n pieces $[T_{j-1}, T_j]$ with $T_j = \frac{j}{n}T$ ($0 \leq j \leq n$) and $\tau_j = \frac{T}{n}$: $1 \leq j \leq n$, and the corresponding discrete random variables are denoted by $X_j = X(T_j)$. Then the increments $Y_1 = X_1$ and $Y_j = X_j - X_{j-1}$: $2 \leq j \leq n$ are independent and identically distributed random variables. The underlying distribution \mathcal{F} can be prepared by Grover's method $|0\rangle_s \rightarrow |\mathcal{F}\rangle_j = \sum_{k=1}^S p_j(k) |k\rangle$, where $s = \log S$ is the number of qubits of the approximation $\tilde{\mathcal{F}}_j$ and $p_j(k)$ is the probability amplitude that the random variable X_j lies in the k^{th} interval of $\tilde{\mathcal{F}}$ with $\sum_{k=1}^S p_j^2(k) = 1$ (see [19] for reference). The circuit depth of the preparation of $\tilde{\mathcal{F}}$ is at most s utilizing S control-rotation gates.

Then the increments sequence Y_j : $1 \leq j \leq n$ can be derived by repeating this procedure on n parallel subcircuits: $|Y_1\rangle |Y_2\rangle \dots |Y_n\rangle = \bigotimes_{j=1}^n |\mathcal{F}\rangle_j$. The desired path variables $\{X_j = \sum_{j'=1}^j Y_{j'} : 1 \leq j \leq n\}$ are derived by a sequence of recursive add operators on these n registers as $|Y_1\rangle |Y_2\rangle \dots |Y_n\rangle \rightarrow |Y_1\rangle |Y_1 \oplus Y_2\rangle |Y_3\rangle \dots |Y_n\rangle \rightarrow \dots \rightarrow |Y_1\rangle |Y_1 \oplus Y_2\rangle \dots |Y_1 \oplus Y_2 \oplus \dots \oplus Y_n\rangle = |X_1, X_2, \dots, X_n\rangle$ (See FIG. 4 (c)). Each add operator takes $2 \log(nS) - 1$ Toffoli gates and $5 \log(nS) - 3$ C-NOT gates. A simple computation shows that the circuit depth is $S + (n-1)(2 \log(nS) + 4) = O(S + n \log(nS))$ and the gate complexity is at most $nS + (n-1)(5 \log nS - 3 + 2 \log nS - 1) = O(n(S + \log(nS)))$ gates. \square

3. Proof of Corollary 3 and Corollary 4

Proof. By definition of Poisson Point Process, the distinct increments Y_j : $1 \leq j \leq n$ are constant 1, and the X_j varies exactly from 1 to n so that the adder subcircuit introduced in Theorem 2 can be omitted. As a consequent, each X_j can be prepared parallel on at most $\log n$ qubits via $\log n$ rotation gates. And meanwhile the holding times τ_j : $1 \leq j \leq n$ are assumed to follow an exponential distribution $\mathcal{F}(\lambda)$, and can thus be prepared parallel, by Theorem 1, on $\frac{-\ln \epsilon}{\lambda}$ qubits via $\frac{-\ln \epsilon}{\lambda}$ rotation gates with circuit depth 1. In summary, the qubit number, circuit depth and gate complexity are respectively $n \log n + n \frac{-\ln \epsilon}{\lambda} = n \lceil \log(\frac{-n \ln \epsilon}{\lambda}) \rceil$, $\max\{\lceil \log n \rceil, 1\} = \lceil \log n \rceil$, and $n \log \frac{-\ln \epsilon}{\lambda} + \sum_{j=1}^n \log j = O(n \lceil \log(\frac{-n \ln \epsilon}{\lambda}) \rceil)$. As for the case of Compound Poisson Process, the only difference is the I.I.D. state space of jumps. Another $n \lceil \log S \rceil$ qubits are introduced to record these jumps, and hence the qubits number turn to be $n \lceil \log(\frac{-nS \ln \epsilon}{\lambda}) \rceil$. Instead of copies of Hadamard gates in *Poisson point process*, a sequence of $n-1$ adder operators are needed, asking for $(n-1)(2 \lceil \log(nS) \rceil - 1)$ Toffoli gates and $(n-1)(5 \lceil \log(nS) \rceil - 3)$ C-NOT gates. Thus the total gate complexity is $O(n \lceil \log(\frac{-nS \ln \epsilon}{\lambda}) \rceil)$, and the circuit depth is $S + n \lceil \log(nS) \rceil$. \square

4. Proof of Theorem 5

Proof. Assuming that the n pieces of the *continuous Markov process* are (X_j, τ_j) , and the j^{th} transition time are $T_j = \sum_{j'=1}^j \tau_{j'}$, a direct computation shows that

$$\begin{aligned}
& \mathbb{P}[X_{j+1} = k_{j+1} | \wedge_{j'=1}^j X_{j'} = k_{j'}] \\
&= \mathbb{P}[X(T_j) = k_{j+1} | \wedge_{j'=1}^j X(t) = k_{j'} : T_{j'-1} \leq t < T_j] \\
&= \mathbb{P}[X(T_j) = k_{j+1} | X(t) = k_j : T_{j-1} \leq t < T_j] \\
&= \mathbb{P}[X_{j+1} = k_{j+1} | X_j = k_j].
\end{aligned} \tag{B8}$$

This reveals that X_{j+1} is totally determined by the previous state X_j with the transition probabilities $P_{kl} =$

$P(X_{j+1} = k | X_j = l)$, and thus the embedded sequence $\{X_j : 1 \leq j \leq n\}$ is a discrete Markov chain as claimed above. By the Markov condition again, the holding time τ_j satisfies

$$\mathbb{P}[\tau_j > t + s | \tau_j > t] = \mathbb{P}[\tau_j > s]. \quad (\text{B9})$$

Noticing that Eq.(B9) is exactly the memory-less condition in Theorem 1, and therefore τ_j follows an exponential distribution with the λ_j determined by the current state X_j . As a consequence of the embedded discrete Markov chain and the exponential distribution holding time, a quantum *continuous Markov process* state can be prepared as follows: $n \lceil \log S \rceil$ qubits are introduced for the storage of the discrete Markov chain, and another $n \lceil \log(-\frac{1}{\lambda_{\min}} \ln \epsilon) \rceil$ qubits are introduced for the holding time τ_j . The initial state $|X_1\rangle = \sum_{k=1}^S p(k) |k\rangle$ is derived by S control-rotation gates via Grover's state preparation method. Following that, $n - 1$ successive transition matrix operators, each of which consists of S^2 multi-controlled rotation gates, are applied to generate $|X_j\rangle : 2 \leq j \leq n$. The n holding times can be prepared parallel, and each τ_j needs at most s different exponential distribution with $S \lceil \log(-\frac{1}{\lambda_{\min}} \ln \epsilon) \rceil$ gates and S circuit depth. In summary, the total number of gates is $S + (n - 1) * S^2 + n * S \lceil \log(-\frac{1}{\lambda_{\min}} \ln \epsilon) \rceil = O(nS \lceil S + \log(-\frac{\ln \epsilon}{\lambda_{\min}}) \rceil)$, and the circuit depth is $S + (n - 1) * S^2 + n * S = O(nS^2)$. \square

5. Proof of Theorem 6

Proof. As shown in FIG. 6, the preparation can be divided into two steps: Firstly, the stochastic process of intensity $\lambda(t)$ is prepared on parallel $n * q_{\mathcal{F}}$ qubits, and the circuit depth is $O(d_{\mathcal{F}})$ as given. Secondly, the holding time τ_j is prepared by a sequence of controlled- V operators. Given a piece of Cox process and the corresponding fixed intensity λ , the holding time follows an exponential distribution as described in Theorem 1 so that it can be prepared within 1 circuit depth by rotation angles $\theta_j = \tilde{\epsilon}^{1/2^{j+1}} : 1 \leq j \leq m$, where $\tilde{\epsilon} = e^{-\lambda T}$. As for varying digital-encoded $\lambda = |l_1, l_2, \dots, l_{q_{\mathcal{F}}}\rangle$, it can be divided into $2_{q_{\mathcal{F}}}$ sequences of controlled-rotation gates with $2_{q_{\mathcal{F}}}$ circuit depth. Hence the total circuit depth for preparing τ_j is $d_{\mathcal{F}} + 2_{q_{\mathcal{F}}}$. On the other hand, the preparation of increments Y_j can be implemented parallel with $d_{\mathcal{G}}$ circuit depth. Thus the circuit depth of the preparation is $\max\{d_{\mathcal{F}} + 2_{q_{\mathcal{F}}}, d_{\mathcal{G}}\}$. To derive X_j or T_j , n addresses are needed, with $nd_{\mathcal{G}}$ or $-\frac{n \ln \epsilon}{\lambda_{\min}}$, respectively. \square

Appendix C: Proofs for Information Extraction Problem

1. Proof of Theorem 7

Proof. A direct computation shows that:

$$I(X, T) = \int_{t=0}^T X(t) dt = \sum_{j=0}^n X_j \tau_j. \quad (\text{C1})$$

The expected value of Eq.(C1) is evaluated as:

$$\begin{aligned} \mathbb{E}[f(I(X, T))] &= \sum_{X(t) \in \Omega_n} f\left(\int_{t=0}^T X(t) dt\right) \mathbb{P}[X(t)] \\ &= \sum_{X(t) \in \Omega_n} f\left(\sum_{j=0}^n X_j \tau_j\right) \mathbb{P}[X(t)] \\ &= \sum_{X(t) \in \Omega_n} f\left(\sum_{j=0}^n Z_j\right) \mathbb{P}[X(t)], \end{aligned} \quad (\text{C2})$$

where $Z_j = X_j \tau_j$ can be derived via a quantum multiplication circuit introduced in Lemma 9 with complexity $O(l_x l_\tau)$. The total circuit depth is $O(\mathcal{P} + nl_x l_\tau)$ (as shown in FIG. 7 (c)). Noticing that the variables of f in Eq.(C2) can be evaluate through a standard procedure (one can see [24] for reference). To guarantee the theoretical closure, we shall sketch this procedure as follows. Suppose that the function f can be truncated on an interval of length P , then it can be extended to a P -periodic function f_P . The Fourier approximation of order L for f_P is denoted by $f_{P,L}(x) = \sum_{l=-L}^L c_l e^{i \frac{2\pi l}{P} x}$, then Eq.(C2) is evaluated as

$$\begin{aligned} \mathbb{E}[f_{P,L}(I(X, T))] &= \mathbb{E}[f_{P,L}\left(\sum_{j=0}^n Z_j\right)] \\ &= \sum_{l=-L}^L c_l \mathbb{E}\left[e^{i \frac{2\pi l}{P} (\sum_{j=1}^n Z_j)}\right] \\ &= \sum_{l=-L}^L c_l \left(\mathbb{E}\left[\cos\left(\frac{2\pi l}{P} \left(\sum_{j=1}^n Z_j\right)\right)\right] + i \mathbb{E}\left[\sin\left(\frac{2\pi l}{P} \left(\sum_{j=1}^n Z_j\right)\right)\right]\right), \end{aligned} \quad (\text{C3})$$

Each term $\mathbb{E}\left[\cos\left(\frac{2\pi l}{P} \left(\sum_{j=0}^n Z_j\right)\right)\right]$ and $\mathbb{E}\left[\sin\left(\frac{2\pi l}{P} \left(\sum_{j=1}^n Z_j\right)\right)\right]$ in Eq.(C3) can be evaluated via the standard amplitude estimation algorithm. Given the error bound ϵ , the circuit should be repeated $O(1/\epsilon)$ times for each term. The total time complexity is hence $O\left(\frac{LP}{\epsilon} (\mathcal{P} + nl_x l_\tau)\right)$ \square

2. Proof of Theorem 8

Proof. A direct computation shows that:

$$\begin{aligned} J(X, T) &= \int_{t=0}^T g(t)X(t) dt \\ &= \sum_{j=1}^n X_j G_j \\ &= \sum_{j=1}^n \left(\sum_{j'=1}^j Y_{j'} \right) G_j \end{aligned}$$

where $G_j = \int_{T_{j-1}}^T g(t) dt$ is a piece-wise integral on the interval $[T_{j-1}, T]$ with $T_j = \sum_{j'=1}^j \tau_{j'}$ and $T_0 = 0$, and $Y_{j'}$ is the j'^{th} increment. By exchanging the order of summation, one have that:

$$\begin{aligned} J(X, T) &= \sum_{j'=1}^n Y_{j'} \left(\sum_{j=j'}^n G_j \right) \\ &= \sum_{j'=1}^n Y_{j'} F(T - T_{j'-1}) \end{aligned} \quad (C4)$$

$$= \sum_{j'=1}^n Y_{j'} G(T_{j'-1}), \quad (C5)$$

where $F(T') = \int_{T-T'}^T g(t) dt$ in Eq.(C4) satisfies:

$$F(T - T_{j'-1}) = \int_{T_{j'-1}}^T g(t) dt = \sum_{j=j'}^n G_j,$$

and $G(T') = \int_{T'}^T g(t) dt$ in Eq.(C5) satisfies:

$$G(T_{j'-1}) = \int_{T_{j'-1}}^T g(t) dt = \sum_{j=j'}^n G_j.$$

Thus the expected value of Eq.(C4) and Eq.(C5) can be evaluated as

$$\begin{aligned} \mathbb{E}[f(J(X, T))] &= \sum_{X(t) \in \bar{\Omega}_n} f\left(\sum_{j=1}^n Y_j F(T - T_{j-1})\right) \mathbb{P}[X(t)] \end{aligned} \quad (C6)$$

$$= \sum_{X(t) \in \bar{\Omega}_n} f\left(\sum_{j=1}^n Y_j G(T_{j-1})\right) \mathbb{P}[X(t)] \quad (C7)$$

$$= \sum_{X(t) \in \bar{\Omega}_n} f\left(\sum_{j=1}^n W_j\right) \mathbb{P}[X(t)]. \quad (C8)$$

The state $F(T - T_{j'-1})$ in Eq.(C6) is a function of the variable $T - T_{j'-1}$, and hence can be computed via a operator F on the $T - T_{j'-1}$ qubit as illustrated in FIG. 7 (d). And the directed area $W_j = Y_j F(T - T_{j-1})$ can be derived through a quantum multiplier introduced in Lemma 9 with complexity $O(l_x l_T)$. In the same way the state $G(T_{j'-1})$ in Eq.(C7) is a function of the variable $T_{j'-1}$, and hence can be computed via a operator G on the $T_{j'-1}$ qubit. And the directed area $W_j = Y_j G(T_{j'-1})$ can be derived with complexity $O(l_Y l_T)$ (see FIG. 7 (e) for reference). The total circuit depth is $O(\mathcal{P} + \mathcal{F} + n l_x l_T + n \max(l_x, l_T))$ or $O(\mathcal{P} + \mathcal{G} + n l_Y l_T)$. Noticing that the expression in Eq.(C8) once again take the form of a summation, and thus can be solved through a standard procedure of amplitude estimation as mentioned above: The Fourier approximation of order L for f_P is denoted by $f_{P,L}(x) = \sum_{l=-L}^L c_l e^{i \frac{2\pi l}{p} x}$, then Eq.(C8) is evaluated as

$$\begin{aligned} \mathbb{E}[f_{P,L}(J(X, T))] &= \mathbb{E}[f_{P,L}\left(\sum_{j=1}^n W_j\right)] \\ &= \sum_{l=-L}^L c_l \mathbb{E}[e^{i \frac{2\pi l}{p} (\sum_{j=1}^n W_j)}] \\ &= \sum_{l=-L}^L c_l \left(\mathbb{E}[\cos\left(\frac{2\pi l}{p} (\sum_{j=1}^n W_j)\right)] + i \mathbb{E}[\sin\left(\frac{2\pi l}{p} (\sum_{j=1}^n W_j)\right)] \right). \end{aligned} \quad (C9)$$

Each term $\mathbb{E}[\cos\left(\frac{2\pi l}{p} (\sum_{j=1}^n W_j)\right)]$ and $\mathbb{E}[\sin\left(\frac{2\pi l}{p} (\sum_{j=1}^n W_j)\right)]$ in Eq.(C9) can be evaluated via rotation operators on the target qubit controlled by W_j together with a standard amplitude estimation subcircuit.(as shown in the box in FIG. 7 (d) and FIG. 7 (e). Given the error bound ϵ , the circuit should be repeated $O(1/\epsilon)$ times for each term. The total time complexity is hence $O\left(\frac{LP}{\epsilon} (\mathcal{P} + \mathcal{F} + n l_x l_T + n \max(l_x, l_T))\right)$ or $O\left(\frac{LP}{\epsilon} (\mathcal{P} + \mathcal{G} + n l_Y l_T)\right)$ for holding time and increment representation, respectively. \square

-
- [1] A. Papantoleon, arXiv preprint arXiv:0804.0482 (2008).
- [2] O. E. Barndorff-Nielsen, T. Mikosch, and S. I. Resnick, *Lévy processes: theory and applications* (Springer Science & Business Media, 2001).
- [3] T. M. Liggett, *Continuous time Markov processes: an introduction*, Vol. 113 (American Mathematical Soc., 2010).
- [4] W. J. Anderson, *Continuous-time Markov chains: An applications-oriented approach* (Springer Science & Business Media, 2012).
- [5] A. Dassios and J.-W. Jang, *Finance and Stochastics* **7**, 73 (2003).
- [6] S. M. Ross, J. J. Kelly, R. J. Sullivan, W. J. Perry, D. Mercer, R. M. Davis, T. D. Washburn, E. V. Sager, J. B. Boyce, and V. L. Bristow, *Stochastic processes*, Vol. 2 (Wiley New York, 1996).
- [7] Y. V. Kozachenko, O. O. Pogorilyak, I. V. Rozora, and A. M. Tegza, *Simulation of stochastic processes with given accuracy and reliability* (Elsevier, 2016).
- [8] R. P. Feynman, *Optics news* **11**, 11 (1985).
- [9] D. P. DiVincenzo, *Fortschritte der Physik: Progress of Physics* **48**, 771 (2000).
- [10] F. Arute, K. Arya, R. Babbush, D. Bacon, J. C. Bardin, R. Barends, R. Biswas, S. Boixo, F. G. Brandao, D. A. Buell, *et al.*, *Nature* **574**, 505 (2019).
- [11] R. Orus, S. Mugel, and E. Lizaso, *Reviews in Physics* **4**, 100028 (2019).
- [12] D. J. Egger, C. Gambella, J. Marecek, S. McFaddin, M. Mevissen, R. Raymond, A. Simonetto, S. Woerner, and E. Yndurain, *IEEE Transactions on Quantum Engineering* (2020).
- [13] S. McArdle, S. Endo, A. Aspuru-Guzik, S. C. Benjamin, and X. Yuan, *Reviews of Modern Physics* **92**, 015003 (2020).
- [14] C. Outeiral, M. Strahm, J. Shi, G. M. Morris, S. C. Benjamin, and C. M. Deane, *Wiley Interdisciplinary Reviews: Computational Molecular Science* **11**, e1481 (2021).
- [15] P. S. Emani, J. Warrell, A. Anticevic, S. Bekiranov, M. Gandal, M. J. McConnell, G. Sapiro, A. Aspuru-Guzik, J. T. Baker, M. Bastiani, *et al.*, *Nature Methods* , 1 (2021).
- [16] H. Ma, M. Govoni, and G. Galli, *npj Computational Materials* **6**, 1 (2020).
- [17] Y. Cao, J. Romero, and A. Aspuru-Guzik, *IBM Journal of Research and Development* **62**, 6 (2018).
- [18] M. Schuld and F. Petruccione, *Supervised learning with quantum computers*, Vol. 17 (Springer, 2018).
- [19] L. Grover and T. Rudolph, arXiv preprint quant-ph/0208112 (2002).
- [20] A. C. Vazquez and S. Woerner, *Physical Review Applied* **15**, 034027 (2021).
- [21] A. G. Rattew and B. Koczor, arXiv preprint arXiv:2205.00519 (2022).
- [22] T. J. Elliott and M. Gu, *npj Quantum Information* **4**, 1 (2018).
- [23] K. Korzekwa and M. Lostaglio, *Physical Review X* **11**, 021019 (2021).
- [24] A. Montanaro, *Proceedings of the Royal Society A: Mathematical, Physical and Engineering Sciences* **471**, 20150301 (2015).
- [25] P. Reberntrost, B. Gupt, and T. R. Bromley, *Physical Review A* **98**, 022321 (2018).
- [26] N. Stamatopoulos, D. J. Egger, Y. Sun, C. Zoufal, R. Iten, N. Shen, and S. Woerner, *Quantum* **4**, 291 (2020).
- [27] A. Martin, B. Candelas, Á. Rodríguez-Rozas, J. D. Martín-Guerrero, X. Chen, L. Lamata, R. Orús, E. Solano, and M. Sanz, arXiv preprint arXiv:1904.05803 (2019).
- [28] S. Woerner and D. J. Egger, *npj Quantum Information* **5**, 1 (2019).
- [29] C. Blank, D. K. Park, and F. Petruccione, *npj Quantum Information* **7**, 1 (2021).
- [30] V. Giovannetti, S. Lloyd, and L. Maccone, *Physical review letters* **100**, 160501 (2008).
- [31] V. Giovannetti, S. Lloyd, and L. Maccone, *Physical Review A* **78**, 052310 (2008).
- [32] F.-Y. Hong, Y. Xiang, Z.-Y. Zhu, L.-Z. Jiang, and L.-N. Wu, *Physical Review A* **86**, 010306 (2012).
- [33] D. Lando, *Review of Derivatives research* **2**, 99 (1998).
- [34] R. C. Merton, *The American Economic Review* **88**, 323 (1998).
- [35] Y.-K. Kwok, *Mathematical models of financial derivatives* (Springer Science & Business Media, 2008).
- [36] F. Black and M. Scholes, in *World Scientific Reference on Contingent Claims Analysis in Corporate Finance: Volume 1: Foundations of CCA and Equity Valuation* (World Scientific, 2019) pp. 3–21.
- [37] R. C. Merton, *Journal of financial economics* **3**, 125 (1976).
- [38] H. U. Gerber and E. S. Shiu, *North American Actuarial Journal* **2**, 48 (1998).
- [39] M. B. Garman, *Journal of financial Economics* **3**, 257 (1976).
- [40] A. Madhavan, *Journal of financial markets* **3**, 205 (2000).
- [41] H. U. Gerber and E. S. Shiu, *Insurance: Mathematics and Economics* **24**, 3 (1999).
- [42] S. A. Cuccaro, T. G. Draper, S. A. Kutin, and D. P. Moulton, arXiv preprint quant-ph/0410184 (2004).